UNIVERZITA KARLOVA V PRAZE
FARMACEUTICKÁ FAKULTA V HRADCI KRÁLOVÉ
Katedra biochemických věd

UNIVESITY OF GOTHENBURG
FACULTY OF SCIENCE
Department of Chemistry and Molecular Biology

CELL-FREE EXPRESSION OF A VOLTAGE-GATED SODIUM CHANNEL FOR FUTURE 2D IR SPECTROSCOPIC STUDIES

BEZBUNĚČNÁ EXPRESE NAPĚŤOVĚ ŘÍZENÉHO SODÍKOVÉHO KANÁLU PRO BUDOUCÍ 2D IR SPEKTROSKOPICKÉ STUDIE

Master Thesis/ diplomová práce

Supervisor/ školitel: Dr. Sebastian Peuker

Prof. RNDr. Lenka Skálová, Ph.D.

Gothenburg 2014

Gabriela Kovácsová

"I declare that I have developed and written this Master Thesis completely by myself. Any thoughts from others or literal quotations are listed in the bibliographical section and properly cited in the text. The Master Thesis was not used in the same or in a similar version to achieve another academic grading."

„Prohlašuji, že tato práce je mým původním autorským dílem. Veškerá literatura a další zdroje, z nichž jsem při zpracování čerpala, jsou uvedeny v seznamu použité literatury a v práci řádně citovány. Práce nebyla využita k získání jiného nebo stejného titulu."

Hradec Králové 2014 Gabriela Kovácsová

Dedicated to the memory of my grandma and grandpa Agnesa and Vendelín Kovács

Special thanks go to Dr. Sebastian Peuker. I am very grateful for all the time and energy he spent on guiding me through this fascinating project, from the first experiment until the very last proofreading of my thesis. He allowed me to grow as a science student by encouraging me to think and by telling me what to do, but first letting me find out how myself. I really appreciate this whole experience and even though it was not always a piece of cake, I enjoyed it and I learned a lot, including some funny old German sayings (jetzt ist der Drops schon wirklich gelutscht!).

I am extremely thankful to Assoc. Prof. Sebastian Westenhoff Ph.D. for accepting me in his group, for making all this possible and for his enthusiastic support. I could not have asked for a better group leader.

Acknowledgement also goes to Dr. Anders Pederson for the CFPE protocol and to Prof. Daniel L. Minor PhD for the provided DNA material and help with the HRV 3C protease protocol.

I thank all the members of the Department of Chemistry and Molecular Biology for their help whenever needed and for all the nice fikas and lunch breaks, which would make the day so much better.

I wish to express my gratitude to Prof. RNDr. Lenka Skálová, Ph.D. for taking me under her wings.

I am grateful to Prof. RNDr. Petr Solich, CSc. and Ing. Hana Krieglerová for enabling my Erasmus Programme stay.

Last but not least, I am much obliged to my parents for their tireless support and faith, to my grandmas for their prayers and to my close ones for distraction whenever needed.

ABSTRAKT

Univerzita Karlova v Praze
Farmaceutická fakulta v Hradci Králové
Katedra biochemických věd

Kandidát: Gabriela Kovácsová
Školitel: Dr. Sebastian Peuker, Prof. RNDr. Lenka Skálová, Ph.D.
Název diplomové práce: Bezbuněčná exprese napěťově řízeného sodíkového kanálu pro budoucí 2D IR spektroskopické studie

Napěťově řízené sodíkové kanály (Na_v), membránové proteiny z nadrodiny napěťově řízených iontových kanálů, jsou součástí každé excitabilní buňky, kde se podílejí na propagaci akčních potenciálů změnou propustnosti její membrány pro sodíkové ionty. Eukaryotní Na_v jsou tvořeny jedním pseudo-homotetramerickým polypeptidem, ve kterém se čtyřikrát opakuje šest transmembránových segmentů (S1-S6). S1-S4 tvoří napěťový senzor reagující na změny napětí na membráně a S5 spolu s S6 tvoří samotný pór kanálu, na jehož extracelulárním ústí je selektivní filtr rozeznávající sodíkové ionty. Zatímco iontová selektivita napěťově řízených draselných kanálů byla detailně popsána na molekulární úrovni, málo je známo o principu selektivity u Na_v.
Studie selektivního filtru pomocí 2D IR spektroskopie, což je metoda schopná poskytnout strukturní informace o daných vazebných interakcích s časovým rozlišením na pikosekundy až milisekundy, vyžaduje velké množství vyčištěného proteinu. To je těžké získat v případě eukaryotních Na_v, a proto jsme jako model zvolili pór prokaryotního Na_v ze *Silicibacter pomeroy* (Na_vSp1p). 2D IR studie dále vyžadují vzorky, kde je izotopicky značena jen zvolená vazba a takové vzorky lze připravit pouze expresí v bezbuněčném systému.
V této práci prezentujeme první bezbuněčnou expresi napěťově řízeného sodíkového kanálu a jeho následnou purifikaci. Pro přípravu izotopově značených vzorků jsme vybrali tři aminokyseliny, které se s největší pravděpodobností podílejí na iontové selektivitě Na_vSp1p a jejich sekvence byla zmutována na terminační kodon TAG, což povede k inkorporaci izotopově značené aminokyseliny. Toto umožní 2D IR spektroskopické studie a pomůže objasnit princip sodíkové selektivity napěťově řízených sodíkových kanálů.

ABSTRACT

Charles University in Prague
Faculty of Pharmacy in Hradec Králové
Department of Biochemical Sciences

Candidate: Gabriela Kovácsová
Supervisor: Dr. Sebastian Peuker, Prof. RNDr. Lenka Skálová, Ph.D.
Title of diploma thesis: Cell-free expression of a voltage-gated sodium channel for future 2D IR spectroscopic studies

Voltage-gated sodium channels (Na_vs) are membrane proteins from the superfamily of voltage-gated ion channels (VGIC), and are present in every excitable cell where they participate in the propagation of action potentials by changing the Na^+ permeability of the cell membrane. Eukaryotic Na_vs are pseudo homotetrameric polypeptides, comprising four repeats of six transmembrane segments (S1-S6), where S1 to S4 form the voltage-sensing domain and S5 and S6 create the pore domain with the selectivity filter on the extracellular site. Whereas the ion selectivity of the voltage-gated potassium channels has been elucidated on the molecular level in great detail, little is known about this for the voltage-gated sodium channels.

To allow future studies of the selectivity filter of Na_v by the means of 2D IR spectroscopy, a technique able to provide bond-specific structural information on the picosecond to millisecond time scales, large quantities of the purified channel are needed. Eukaryotic Na_vs are difficult to obtain in these amounts. Therefore we have chosen a prokaryotic pore-only Na_v from *Silicibacter pomeroy* (Na_vSp1p) as a model system. Furthermore, 2D IR studies require site-specifically isotope labeled samples which can only be produced in cell-free expression systems.

In this work, we report the first cell-free expression of a voltage-gated sodium channel and its subsequent purification. To prepare the isotope labeling, three amino acids, which are most likely involved in the ion selectivity of Na_vSp1p, were identified and mutated to amber codons. This will allow 2D IR spectroscopy studies and will help to reveal the principle of sodium ion selectivity in Na_vs.

CONTENTS

1 INTRODUCTION

This work is a part of a more extensive project aiming to investigate the ion selectivity of voltage-gated sodium channels by 2D IR spectroscopy using site-specifically isotope-edited proteins. Voltage-gated sodium channels (Na_v) are membrane proteins from the superfamily of voltage-gated ion channels (VGIC), closely related to voltage-gated potassium channels and voltage-gated calcium channels (Hille, 2001). As most VGICs, Na_vs comprise six transmembrane segments (S1-S6), where S1 to S4 form the voltage-sensing domain (VSD) and S5 and S6 create the pore domain (PD). Four of these subunits arrange around a central pore to form a functional channel. In contrast to bacterial sodium channels, higher organisms form these channels from single polypeptides. Na_vs are present in every excitable cell as they are involved in the propagation of action potentials by changing Na^+ permeability of the cell membrane (Catterall, 2000). Whereas the ion selectivity of the voltage-gated potassium channel has been already elucidated on the molecular level in great detail, little is known about this for the voltage-gated sodium channels.

2D IR spectroscopy studies require large quantities of purified protein difficult to obtain from eukaryotic sources. However, prokaryotic Na_vs share 20-25% sequence similarity with the eukaryotic Na_vs and therefore are thought to be their ancestors. To simplify the system even further we have worked with the PD of a Na_v from *Silicibacter pomeroyi* (Na_vSp1p), because it has been demonstrated that it folds independently of VSD to a functional channel with the selectivity for sodium ions. At the same time, it is more stable and expresses at higher levels than the complete channel (Shaya et al., 2011). Site-specific isotope labeling, a method that is currently being developed by the Westenhoff group, requires cell-free expression (CFPE) of the protein of interest (Isaksson et al., 2012). Therefore I have developed a method for CFPE and purification of Na_vSp1p. Also, based on recently revealed structures of closely related bacterial Na_vs (Shaya et al., 2013), I have selected three amino acids which are likely to be involved in the selectivity filter of Na_vSp1p and performed a single amino acid mutation in order to incorporate the same, but isotope labeled amino acids ($^{13}C=^{18}O$) in the future. The carbonyl of the isotope labeled amino acid will have a red shifted vibrational frequency in the IR spectrum, which will spectrophotometrically isolate it from the main band of carbonyls of other amino acids and thus enable to study the interactions of this one amino acid (Baiz et al., 2012).

2 THEORETICAL BACKGROUND

2.1 Voltage-gated sodium channels – from Kraken to crystals

Family of voltage-gated ion channels

Ion channels are macromolecular pores in the plasma membrane of eukaryotic and prokaryotic cells that allow passage of ions in and out of the cell. Among their known functions is establishing a resting membrane potential, shaping electrical signals, gating the flow of messenger Ca^{2+} ions, controlling the cell volume, and regulating the net flow of ions and fluids across epithelial cells of secretory and resorptive tissues (Hille, 2001). Ion channels can be classified by different properties, e.g. gating mechanism. IUPHAR (International Union of Basic and Clinical Pharmacology) distinguishes between ligand-gated and voltage-gated ion channels (VGICs). The superfamily of VGICs consists of voltage-gated K^+ channels (K_vs), voltage-gated Na^+ channels (Na_vs), voltage-gated Ca^{2+} channels (Ca_vs), transient receptor potential (TRP) channels (cation channels, diverse in terms of activation mechanism and selectivity with a critical role in sensory physiology and in humans, their mutation underlies diseases (Venkatachalam & Montell, 2007)), cyclic-nucleotide-gated channels (cAMP and cGMP gated nonselective cation channels whose function has been firmly established in rod and cone photoreceptors, in extraretinal photoreceptors, and in sensory neurons of the olfactory epithelium (Kaupp & Seifert, 2002)) and CatSper and Two-Pore channels (calcium-selective channels localized in the plasma membrane of the sperm tail and putative cation-selective ion channels respectively (Clapham & Garbers, 2005)). Sodium channels were discovered first, but in evolution, they are the most recent member of the VGIC superfamily. They arose from closely related Ca_vs and share a topology of 24 transmembrane segments organized in four homologous six-transmembrane repeats. Ca_vs in turn evolved by two rounds of gene duplication from ancestors of K_vs (which form a homotetramer from single domain polypeptides) and cyclic-nucleotide-gated channels (Yu & Catterall, 2003).

Discovery of voltage-gated Na^+ channels (Na_vs)

Recordings of sodium currents were first presented in the classical work of Hodgkin & Huxley (1952), where they studied the plasma membrane of a giant squid axon with voltage clamp techniques. From their experimental data they concluded that responses of the isolated giant axon to electrical stimuli were due to reversible alterations in sodium and potassium permeability arising from changes in membrane potential and they derived equations describing many of its electric properties with fair accuracy. They also observed the three key features that became characteristic for the Na_vs: (1) voltage-dependent activation, (2) rapid inactivation, and (3) selective ion conductance and they defined the three states of Na_vs - open, inactivated and closed. In the 1980s, progressive development of biochemical methods for measurement of ion flux through Na_vs, high affinity binding of neurotoxins to Na_vs, and detergent solubilization and purification of Na_v proteins labeled by neurotoxins led to discovery of the principal α and auxiliary β subunits of Na_vs and revealed that the purified sodium channel contains a functional pore with voltage-dependent activation. Primary structure determination suggesting a large protein with four internally homologous α-helical domains followed, together with functional expression and molecular modeling of the α subunit. This predicted six α-helical transmembrane segments (S1–S6) in each of the four homologous domains (I-IV) and a reentrant loop between helices S5 and S6 which was embedded into the transmembrane region and formed the outer pore and further loops as shown in Fig. 1. Whereas the homologous-domains motif of the α subunit is the building block of K_vs, Ca_vs and other VGICs, the β subunits are structurally similar to the family of immunoglobulin-like folds containing proteins which makes them unique among ion channel subunits (all reviewed in Catterall, 2000).

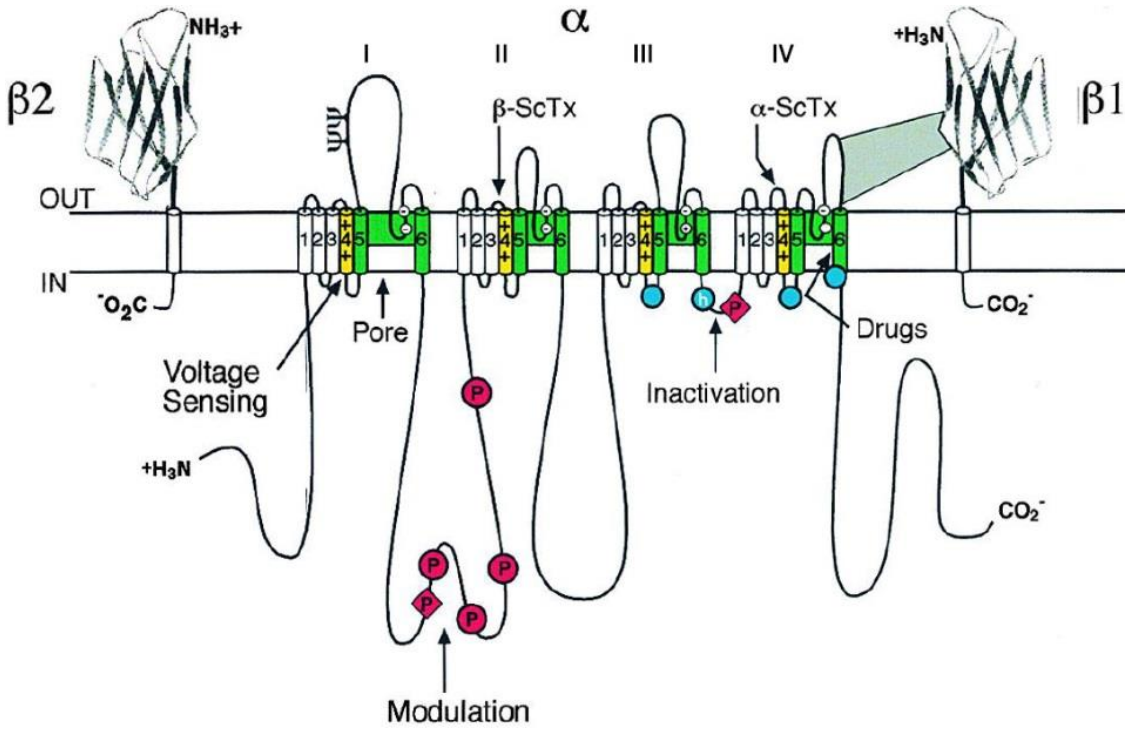

Fig. 1. Schematic representation of a sodium-channel subunits. The α subunit of the $Na_v1.2$ channel is illustrated together with the β1 and β2 subunits; the extracellular domains of the β subunits are shown as immunoglobulin-like folds, which interact with the loops in the α subunits. Roman numerals indicate the domains of the α subunit; segments 5 and 6 (shown in green) are the pore-lining segments and the S4 helices (yellow) make up the voltage sensors. Blue circles in the intracellular loops of domains III and IV indicate the inactivation gate IFM motif and its receptor (h, inactivation gate); P, phosphorylation sites (in red circles, sites for protein kinase A; in red diamonds, sites for protein kinase C); ψ, probable *N*-linked glycosylation site. The circles in the re-entrant loops in each domain represent the amino acids that form the ion selectivity filter (the outer rings have the sequence EEDD and inner rings DEKA). Adapted from Catterall (2000).

Functional features of Na_vs on a molecular level

Information about selective ion conductance was obtained from studies addressing the pore region composed of S5 and S6 α-helixes. Experiments with highly specific Na_vs inhibitors, the neurotoxins tetrodotoxin and saxitoxin, together with mutational analysis led to the identification of their receptor site, which composes of an inner and outer ring of mostly negatively charged amino acid residues in the outer pore. There is multiple evidence that the inner ring DEKA (Asp-Glu-Lys-Ala, one in domains I-IV each) acts as the selectivity filter as mutations in this ring have a strong effect on selectivity for organic and inorganic monovalent cations. Single mutations of K=>E or A=>E within the DEKA motif lead to a calcium selective channel (Heinemann et al., 1992). The inner pore of Na_vs also hosts a receptor site formed by two amino acids in the IVS6 transmembrane segment to which local anesthetics bind with high affinity if the Na_v is in the inactivated state. It was also revealed that Na_vs blocking drugs used as

antiarrhythmics and anticonvulsants interact with this receptor site and also with nearby amino acids (Catterall, 2000).

As for voltage-gated activation, the structure and function of the S4 transmembrane segment was explored. It contains repeated motifs of a positively charged amino acid residue followed by two hydrophobic residues, potentially creating a cylindrical α-helix with a spiral ribbon of positive charges around it (Fig. 2., left). The negative internal transmembrane electrical field would exert a strong force on these positive charges arrayed across the plasma membrane, pulling them into the cell in a cocked position. The sliding helix (Catterall, 1986) or helical screw (Guy & Seetharamulu, 1986) models of gating propose that these positively charged amino acid residues are stabilized in the transmembrane environment by forming ion pairs with negatively charged residues in adjacent transmembrane segments (Fig. 2, right). Depolarization of the membrane was proposed to release the S4 segments to move outward along a spiral path, initiating a conformational change that opens the pore. Although this model was quite speculative when proposed, subsequent studies have supported the two key features suggested – the stabilizing formation of ion pairs and the outward rotational movement of S4 segments (all reviewed in Catterall, 2000).

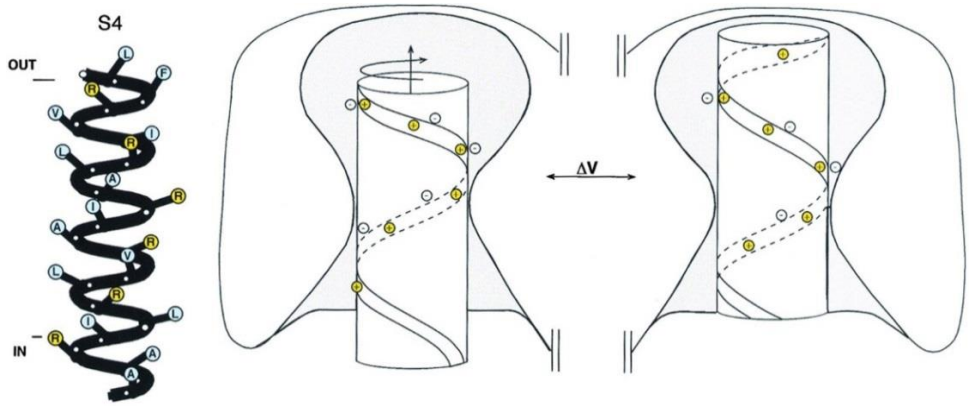

Fig. 2. Voltage-dependent activation by outward movement of the S4 voltage sensors. Left, amino acids in the S4 segments in domain IV of the sodium channel are illustrated in single letter code. Hydrophobic residues are indicated in light blue, and positively charged arginine residues in every third position are highlighted in yellow. Right, a synthesis of the sliding helix or helical screw models of gating (Catterall, 1986; Guy and Seetharamulu, 1986). The S4 segment in a single domain is illustrated as a rigid cylinder within a channel with a narrow, hourglass-shaped waist. Positively charged residues (yellow) are neutralized by interaction with negatively charged residues from the surrounding protein (principally the S2 and S3 segments). Upon depolarization, the segment moves outward and rotates to place the positively charged residues in more outward positions but is still neutralized by interactions with negative residues in the transmembrane part of the protein. Taken from Catterall (2000).

Another important feature of Na_vs is fast inactivation which occurs within milliseconds of opening. In the generally accepted model an inactivation gate formed by the highly conserved sequence IFM in the intracellular loop connecting domains III and IV closes like a hinged-lid the inactivation gate receptor formed by hydrophobic residues in intracellular loops S4-S5 of domains III and IV, as well as the intracellular end of the S6 transmembrane segments of these domains (Fig. 3, Fig. 1) (reviewed in Catterall, 2000).

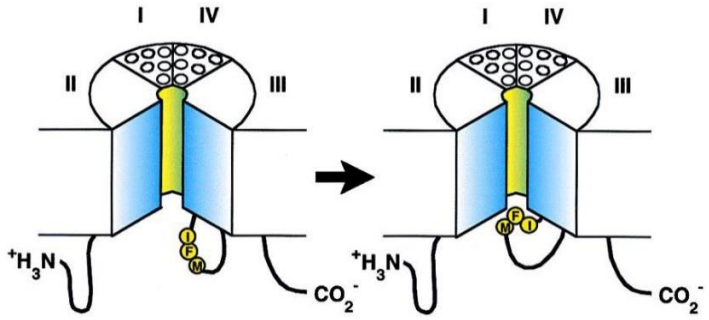

Fig. 3. The hinged-lid mechanism of inactivation of sodium channels. The intracellular loop connecting domains III and IV of the Na_v is depicted as forming a hinged lid. The critical residue Phe-1489 (F) is shown interacting with the inactivation gate receptor at the inner pore of the Na_v during the inactivation process. Adapted from Catterall (2000).

Na_vs in mammalian physiology and pathology

As Na_vs play a crucial role in generation and propagation of action potentials in excitable cells, they are expressed in neuronal, neuroendocrine, skeletal muscle and cardiac cells and so far nine α-subunits of Na_vs were functionally characterized, $Na_v1.1$-$Na_v1.9$. Due to their specific roles, they differ in cellular and tissue expression, which also varies during ontogenesis. Various neuromodulations of Na_vs were observed, e.g. phosphorylation by cAMP-dependent protein kinase A or protein kinase C (reviewed in Cantrell & Catterall, 2001). An important tool for the elucidation of their physiological function is provided by investigating the diseases associated with mutations in ion channel genes, termed channelopathies. Inherited or acquired sodium channel dysfunction resulting in excessive sodium conductance can lead to cardiac arrhythmia, epilepsy, and enhanced pain syndromes. Mutations in four α subunits and one β1 subunit were identified in connection with Na_v channelopathies and among these inherited diseases are long QT syndrome 3, potassium aggravated myotonia and paramyotonia congentia. Another example are mutations in the β1 subunit and in IIS4 and IVS4 segments of the α subunit of $Na_v1.1$, that are linked to autosomal dominant generalized epilepsy with febrile seizures plus, supporting the role of VGSCs in controlling epilepsy (Clare et al., 2000). Several Na_vs subtypes are involved in pain and

other neurological disorders, for example $Na_v1.1$ is also associated with migraine and especially $Na_v1.7$ is gaining interest in neuropathic pain research (Mantegazza et al., 2010).

Interactions with toxins and drugs

Neurotoxins were broadly used to identify and explore functions of Na_vs, and to date, the binding sites and mechanisms of action of some neurotoxins are already known. Na_vs can be subdivided by their sensitivity to tetrodotoxin (TTX), a lethal component of puffer fish, into TTX-sensitive and TTX-resistant, and the amino acids responsible for this phenomena were already pointed out. Tetrodotoxin's high toxicity is caused by binding to open channels, whereas drugs used as sodium channel blockers (e.g. phenytoin, lignocaine, lamotrigine) bind and stabilize inactivated channels (state-dependence). This accounts for the selective inhibition during sustained depolarization (voltage-dependence) or repetitive firing (use-dependence), allowing control of excitability without impairment of critical cardiac, neuromuscular, or ordinary sensory functions, and explaining the safety profile of Na_v drugs. Na_vs modulators have empirical origins and arose in two areas - local anaesthetics, leading to antiarrhythmics, and antiepileptic drugs (Clare et al., 2000). Revealing their mechanism of action on a molecular level attracts a lot of attention and opens doors for design of more potent and subtype selective Na_v blockers for various disorders. The molecular basis for class Ib antiarrhythmic inhibition of cardiac sodium channels has been studied in detail and provides useful information for future antiarrhythmics' design (Pless et al., 2011). Further, antiepileptics might also be efficacious in the treatment of migraine, multiple sclerosis, neurodegenerative diseases, and neuropathic pain (Mantegazza et al., 2010). Also, antiarrhytmics such as lignocaine and mexiletine are tested on their efficacy in neuropathic pain in numerous clinical trials. In conclusion, the topic of sodium channel blockers is of great ongoing interest, but currently limited by little information about the specific subtypes and the lack of novel assays compatible with high throughput screening (Sang et al., 2009).

Mysterious bacterial Na_v to shed some light on yet unrevealed mechanisms

An attempt to find CatSper homologs for functional analysis resulted in the identification of a gene from *Bacillus halodurans* encoding a voltage-gated sodium channel (NaChBac), which was the first bacterial Na_v to be functionally characterized

(Ren et al., 2001). Electrophysiological experiments with heterologously expressed NaChBac as well as with subsequently discovered highly similar bacterial sodium channels revealed they are sodium selective, sensitive to Ca_v blockers (apparently pharmacological properties of these Ca_v blockers are not linked to ion selectivity), voltage-gated ion channel and exhibit activation, inactivation, and recovery similar to those of human sodium channels, albeit at 10–100x slower rates (Koishi et al., 2004; McCusker et al., 2011). Bacterial Na_vs are simpler, the homotetrameric channel is assembled from four domains each consisting of a single six-transmembrane segments (6TM) polypeptide, there is a similar selectivity filter, no obvious cytoplasmic inactivation gate, but the same motif of the voltage-sensing S4 segment as is in other VGICs (Ren et al., 2001). Bacterial Na_vs have 20-25% identity with human Na_vs and are expected to have similar overall structures as they have nearly identical hydrophobicity profiles and predicted topologies as each of the pseudo-repeated eukaryotic domains (McCusker et al., 2011). Also, they have sequence and pharmacological characteristics resembling those of Ca_vs, proposing that they are similar to the ancestral single-domain channel from which Ca_vs and Na_vs have arisen (Yu & Catterall, 2003).

Identification of bacterial Na_vs offered new possibilities, because in contrast to eukaryotic Na_vs, whose high-level expression in any systems in the quantities necessary for biophysical or structural characterization has not been reported yet, some bacterial Na_vs were successfully crystalized and provided precious information on structure and function. In order to find a minimalistic sodium channel, McCusker et al. (2011) and Shaya et al. (2011) designed a dissected pore-domain (PD, final transmembrane helices S5,S6) of the whole Na_v protein from *Silicibacter pomeroyi* (Fig. 4). They proved it formed a functional, tetrameric sodium selective channel and on top of that, it is thermally more stable and expresses in *E.coli* at higher levels.

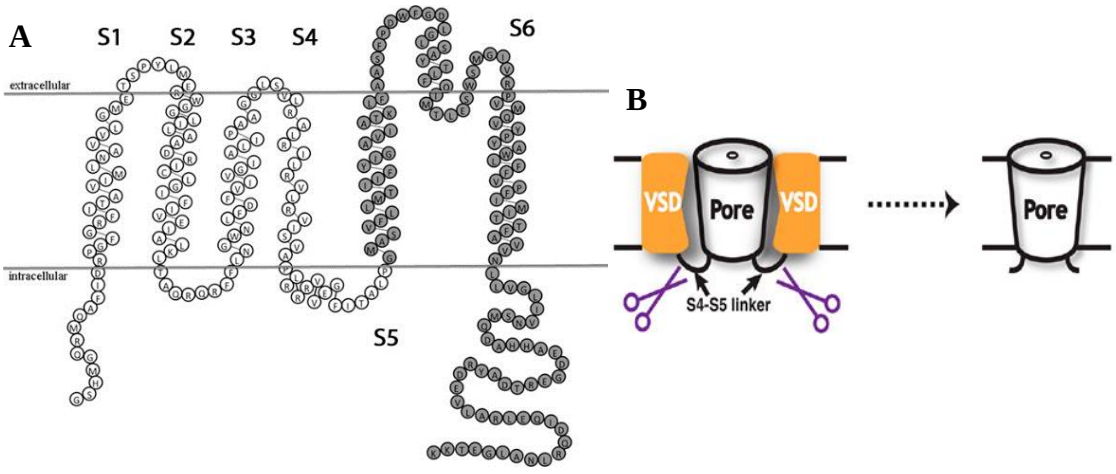

Fig. 4. (*A*) Primary structure of full-length Na_vSp and the pore domain (S5, S6, gray residues), with transmembrane helices marked (S1-S6), adapted from (McCusker et al., 2011). (*B*) Creation of a pore-only Na_v. Two of four voltage-sensing domains (VSD, helices S1-S4) are shown along with the S4-S5 linker connecting them to the pore formed by S5, S6. Scissors indicate the dissection point. Adapted from Shaya et al. (2011).

Shaya et al., (2011) extended the production of PD constructs to Na_vs from *Alcanivorax borkumensis* and *Alkalilimnicola ehrlichei* (Na_vAe1p), the structure of the latter was determined by crystallization (Fig. 5*A,B*) providing detailed information on channel-gating and the structure of the selectivity filter (SF) containing an inner and outer ion binding site, which showed unexpected similarities with Ca_vs and underscored the resemblance between prokaryotic and eukaryotic VGICs (Shaya et al., 2013). The crystal structures of a Na_v S6-cystein mutants from *Arcobacter butzleri* (Na_vAb) provided insight into the molecular basis of voltage-sensing, ion conductance, and voltage-dependent gating (Payandeh et al., 2011), and the crystalized wild type Na_vAb, occurring as a dimer of AB or CD subunit conformations, gave clues about conformational changes that may underlie the process of slow inactivation, a conserved property of Na_vs from bacteria to man (Payandeh et al., 2012). A novel mechanism for channel gating, comprising a movement of the C-terminal end of the S6 helix induced by a simple twist of the backbone, was suggested after crystalizing prokaryotic Na_vs in two different conformational states of the pore – Na_vAb in a hybrid closed conformation (Payandeh et al., 2011) and Na_v from *Magnetococcus sp*. (Na_vMs) in an open conformation (McCusker et al., 2012). The yet unclear mechanism of the ion selectivity filter was studied in detail on crystalized Na_vRh, an ortholog of NaChBac from the marine *alphaproteobacterium* HIMB114 (Fig. 5*C,D*) (Zhang et al., 2012) by the means of molecular dynamics simulations, structural biology and electrophysiological approaches (Zhang et al., 2013). The simulation studies suggest that Na_vRh allows Na^+

permeation in an asymmetric manner with the four chemically identical subunits following independent structural changes, which mimics the mammalian Navs, whose four repeats contain varied sequences in the selectivity filter. The PDs of mentioned structures of homologous bacterial Na_vs are superimposed on each other in Fig. 5*D*.

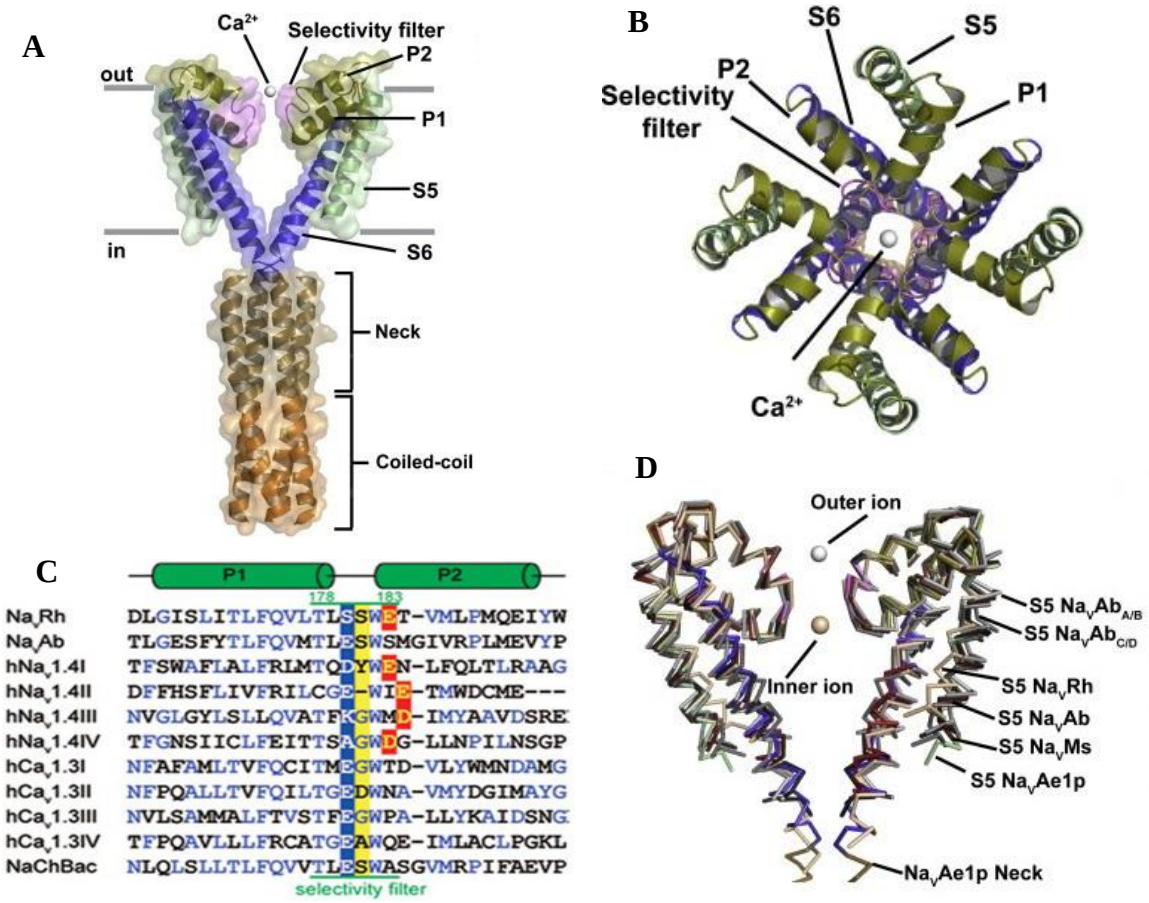

Fig. 5. (*A*) Structure Na_vAe1p, side view showing two transmembrane region subunits and four cytoplasmic tail subunits. Transmembrane helices S5 and S6 are colored green and blue, respectively. P1 and P2 pore helices are colored olive. Selectivity filter is violet. Neck and coiled coil are tan and orange, respectively. Calcium ion is a white sphere. Gray lines show approximate lipid bilayer boundaries. (*B*) Na_vAe1p tetramer extracellular view. Colors are as in *A*. (*C*) The SF sequence of Na_vRh is similar to those of the eukaryotic Na_vs. Sequences of Na_vRh, Na_vAb, NaChBac and human Nav1.4 and Cav1.3 were aligned using ClustalW. The residues in the negatively charged outer and inner rings are shaded red and blue, respectively. Ser181 in Na_vRh and its corresponding residues in other homologs including Tyr407 in hNav1.4I are shaded yellow. (*D*) Backbone superposition of PDs of Na_vAb (black), $Na_vAb_{A/B}$ (light gray), $Na_vAb_{C/D}$ (medium gray), Na_vRh (wheat), Na_vMs (dark red), and Na_vAe1p (colored as in *A*). Outer ion from Na_vAe1p and inner ion from Na_vRh are shown as white and wheat spheres, respectively. Two subunits are shown.as in *A*. The SF of Na_vRh contains two Na^+ binding sites. Pictures *A*,*B*,*D* were adapted from Shaya et al. (2013) and picture C from Zhang et al. (2013).

2.2 Infrared spectroscopy

When a molecule is scanned by infrared light (IR), it will absorb at frequencies which resonate with the vibrational motion of the bonds in the molecule (Fig. 6). The vibrational mode must be associated with a change in the dipole in order to be IR active. The vibrational frequency of a bond is determined by the bond length and by the atomic mass, which makes it possible to detect functional groups of organic molecules in the region between 4000 cm^{-1} to 1500 cm^{-1}, in contrast to absorption in the molecule specific fingerprint region 1500 cm^{-1} to 400 cm^{-1}.

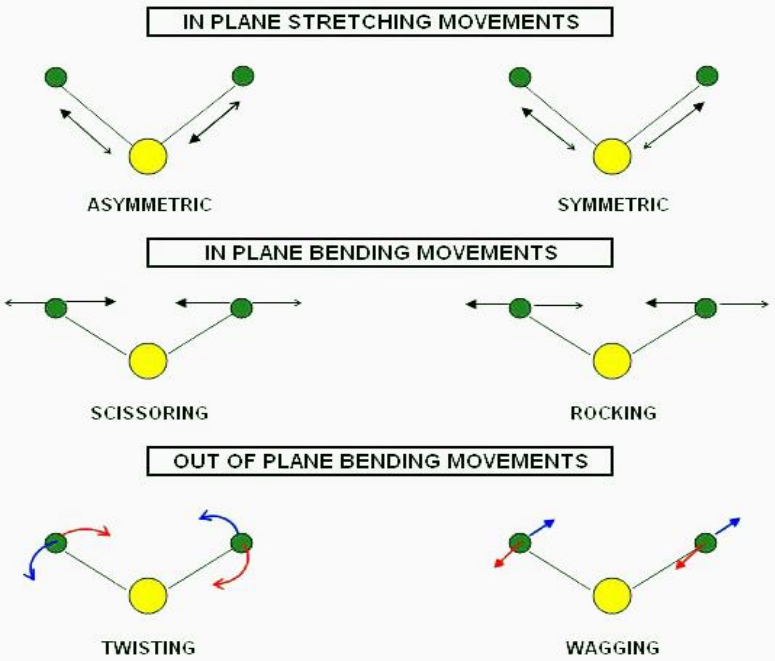

Fig. 6. Examples of vibration modes of CH_2 bonds in a CH_2X_2 molecule. Taken from the online source Fourier Transform Infrared Spectrometry, Intertek.

Most commonly studied vibrational modes in protein IR spectroscopy are amide vibrations of the polypeptide backbone. These comprise amide I vibrations (1600 to 1700 cm^{-1}) and amide II vibrations (around 1550 cm^{-1}). The amide I vibration is a combination of C=O stretching (85%) and N-H in plane bending (10%) of the backbone amide units (Fig. 7*A*) and they give distinct information on secondary structure and hydrogen bonding. α-Helices exhibit a single peak near 1650 cm^{-1}, while β-sheets exhibit two peaks centered near 1630 $cm^{-1}$and 1680 cm^{-1} (Fig. 7*B*). Amide II vibrations derive from C-N bond stretching combined with N-H bending motion (Fig. 7*A*). Deuteration of the solvent red-shifts the peak from 1550 cm^{-1} (Fig. 7*B*) to 1450 cm^{-1} due to hydrogen/deuterium exchange in N-H, which reflects solvent-exposure and conformational flexibility of the protein. However, amide II

modes are less frequently used as they are considered less sensitive to structure and also a variety of side chain absorptions overlaps these bands (Baiz et al., 2012).

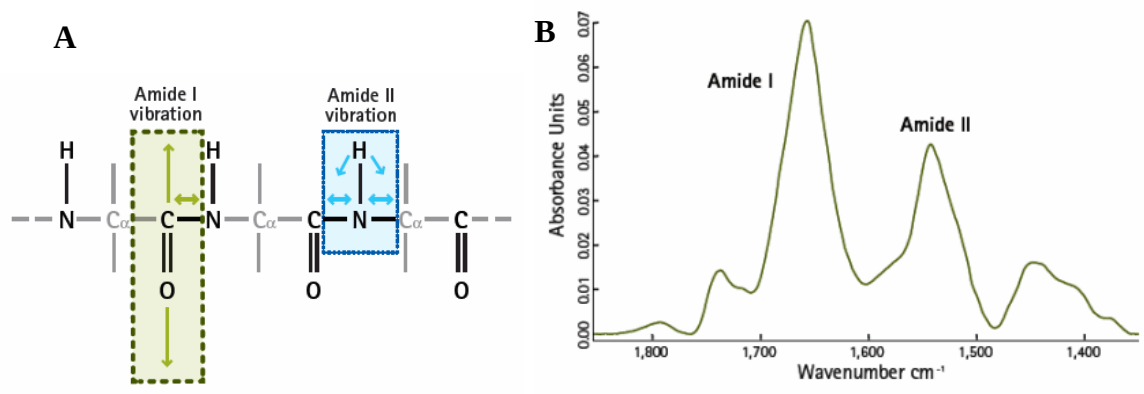

Fig. 7. (*A*) Polypeptide backbone vibrations giving rise to amide I (1600- 1700 cm^{-1}) and amide II (~1550 cm^{-1}) bands in a protein IR spectra (*B*). Picture taken from Direct Detect, Analytical chemistry.

2.2.1 Spectrally isolated sites: hydrogen bonding and isotope labels

IR spectroscopy is one of the few experimental techniques that is sensitive to hydrogen bonding as amide I vibrations red-shift when a hydrogen bond is accepted by the oxygen atom or donated by the hydrogen atom in the amide unit (approximately 16 cm^{-1} shift per one hydrogen bond between the amide oxygen atom and a water molecule). Therefore one can observe solvent-exposed residues having strongly red-shifted frequencies (one oxygen can accept multiple hydrogen bonds) compared to residues locked into stable protein-protein hydrogen bonds. An H-bond reduces the π-orbital overlap CO giving a partial single bond C-O-H character to the C=O···H double bond. The decrease in vibrational frequency can be explained by the increased mass of oxygen and reduced mass of the C=O bond.

Inserting an isotope label enables spectroscopic isolation of a single residue or a small region of interest and aids in determining the local structure and dynamics of the individual residue within a peptide. A single ^{13}C isotope label red-shifts the vibrational frequency of amide I, however, this shift alone may not be sufficient to isolate the residue peak from the main band and therefore a double label $^{13}C=^{18}O$ is needed to provide an ample shift (all from Baiz et al., 2012).

2.2.2 2D IR spectroscopy

2D IR spectroscopy (2D IR) is a nonlinear, vibrational spectroscopy technique able to provide bond-specific structural resolution of molecular systems on picosecond to millisecond time scales. 2D IR spectroscopy spreads a vibrational spectrum over two frequency axes which report on how excitation of a vibration with a given frequency influences all other vibrations within a detection window, following a waiting time. Interpretation of these spectra can be guided by 2D IR spectra computed from molecular dynamics simulations, or by all-atom models.

2D IR can be used to characterize biological processes involving protein conformational change, e.g. enzyme catalysis, transport and signaling, dynamic scaffolding for structures, charge transfer, and mechanical or electrical energy transduction. Furthermore, it can also be used to investigate samples that are difficult to study by traditional techniques, such as protein aggregates and amyloid fibers, intrinsically disordered peptides and membrane proteins (Baiz et al., 2012).

The structural sensitivity of 2D IR stems from *couplings* between vibrational modes that give rise to characteristic infrared bands and *cross-peaks*. Hamm & Zanni (2011) use a simple example to explain the concept of this coupling. Imagine two acetone molecules and their stretching carbonyl bond (Fig. 8). The negative electrons and the positive nuclei create the electronic structure, the molecular orbitals, which dictate the bond length and therefore the vibrational frequencies. Further, the charge distribution of the electrons and the nuclei creates an electrostatic potential, a dipole that surrounds the molecule. If the two acetone molecules are close enough, they will feel one another's potentials, which will slightly alter their molecular orbitals, thereby leading to a shift in the vibrational frequencies. This perturbation, the change in the charge distribution of a molecule when it is vibrationally excited, is termed *transition dipole* and is what couples the vibrational modes. Thus, if we can measure the vibrational coupling and understand its distance and angular dependence, we can determine the distances and orientations of the two molecules with respect to one another. 2D IR spectroscopy provides the measurement, through the cross-peaks, and models provide the structure dependence of the coupling.

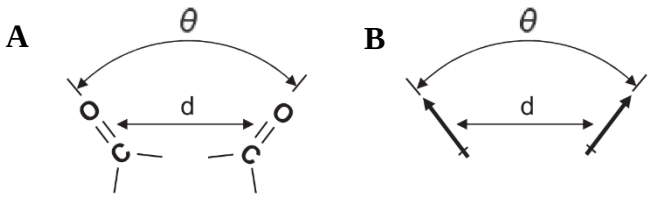

Fig. 8. Two coupled acetone molecules. (*A*) The coupling strength will depend on the distance and orientations. (*B*) Representing the carbonyl stretches with transition dipoles. From Hamm & Zanni, (2011).

Hamm & Zanni (2011) also give a description of a very basic pump-probe experiment generating a 2D IR spectra with cross-peaks. We consider the two acetone molecules, where one is ^{13}C isotope labelled so that the two carbonyl groups, two oscillators, have a different individual vibrational frequency, *local mode frequency*. Local mode states before coupling and eigenstates after coupling are shown in Fig. 9*A*, and Fig. 9*B* shows the resulting 2D IR spectra. We scan the pump frequency (ω_{pump}, *y*-axis) across the resonances of the two oscillators and after a given time, we scan with the probe frequency (ω_{probe}, *x*-axis), and when the pulse comes into resonance with an eigenstate, we mark that frequency along the axes. Each acetone molecule creates a pair of *diagonal peaks* (Fig. 9*B*, pair 3, 4+8 for the higher-frequency oscillator and pair 5, 2+6 for the lower-frequency oscillator). The negative[1], solid contour peak in the pair lies exactly on the diagonal ($\omega_{pump}=\omega_{probe}$) at the fundamental frequency ω_{01} and is composed of two overlapping transitions. We typically measure difference spectra, where absorption of ω_{probe} with the pump pulse switched on is subtracted from ω_{probe} absorption with the pump pulse switched off. This will result in a negative difference spectrum, because after a certain fraction of molecules absorbed ω_{pump} and was excited to the first state, there will be less molecules in the ground state to absorb and be excited to the first state by ω_{probe}, and therefore this absorption of the probe pulse will be smaller than if scanned only with the probe pulse. This is termed a *bleach.* The second transition (4, 6) forming this peak is stimulated emission, also negative. The other, positive peak in the pair (3, 5) arises from excitation from the first to the second state by the subsequent probe pulse and is shifted to a different ω_{probe} frequency, because of the anharmonicity of the carbonyl stretch, and the difference in the frequency is called *diagonal anharmonic shift* (Δ_{11}, Δ_{22}). Since the two molecules are coupled, pairs of cross-peaks appear (7, 8 and 1, 2), which again comprise one negative and one positive peak shifted by the *off-diagonal anharmonic shift* (Δ_{12}, Δ_{21}). The negative cross-peaks 8

[1] To regard this peak as negative is a convention in this book.

and 2 will be observed by the probe pulse as a bleach explained above. Transition 1 excites the lower oscillator by one quantum from its ground state to its first excited state when there is already one quantum of excitation in the higher-frequency oscillator: |01› to |11› and vice versa applies for the transition 7. The existence of a cross-peak in a 2D IR spectrum is a direct manifestation of the coupling between both oscillators. In this context coupling means that the transition frequency of the one oscillator depends on the excitation level of the other oscillator. The off-diagonal anharmonicity Δ_{12} can directly be read off from a 2D IR spectrum, as depicted in Fig. 9*B*.

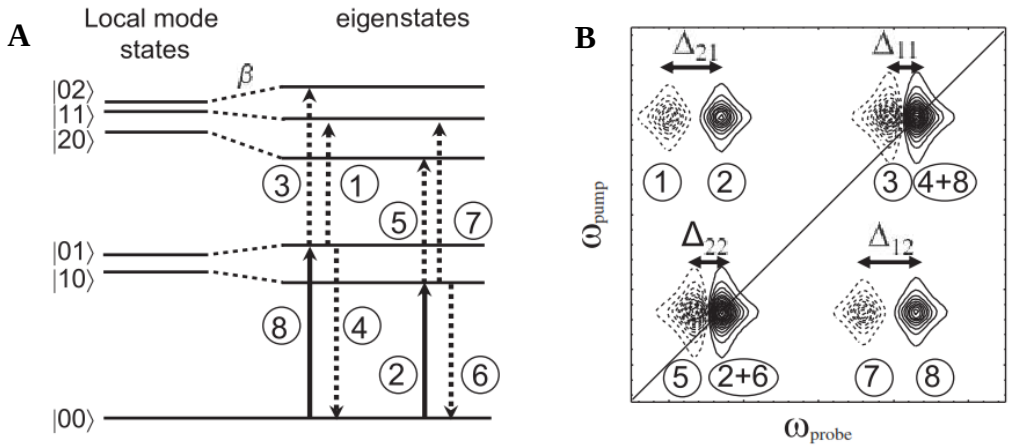

Fig. 9. (A) Level scheme of two coupled oscillators before coupling (local modes) and after coupling (eigenstates). The dipole-allowed transitions are depicted. The solid arrows represent the pump process, the dotted arrows the probe process. (B) Resulting 2D IR spectrum. Solid contour lines represent negative response (bleach and stimulated emission), dotted contour lines positive response (excited state absorption). The labels 1–8 relate each peak in the 2D IR spectrum to the corresponding transition in the level scheme. Taken from Hamm & Zanni (2011).

2.3 Cell-free protein expression

Cell-free protein expression (CFPE) is an *in vitro* synthesis of a desired protein, encoded by an exogenous template DNA added to the transcription and translation machinery extracted from a cell lysate, prokaryotic (e.g. *Escherichia coli*) or eukaryotic (e.g. rabbit reticulocyte, wheat germ). As there is no cell membrane and expression takes place in an entirely open system within a few hours, CFPE rather resembles a complex and coupled chemical reaction than lengthy cell cultivation for *in vivo* overexpression. There is the possibility to directly influence expression conditions as a given added reagent has direct contact with the nascent polypeptide chain and can be used as long as it does not interfere with the system, including chaperonins, cofactors, lipids, detergents and redox buffers, effectively making cell-free synthesis the most versatile expression system currently available. Moreover, there is the practical aspect in setting up expression in small volumes in parallel reaction conditions for screening and optimization purposes. However, to maintain production of proteins from unstable transcripts or proteins susceptible for proteolysis, the presence of RNAse and protease inhibitors is crucial for this vulnerable system (Pedersen et al., 2011).

The protocols for CFPE derived from *E.coli* cells vary in the extract preparation and in the reaction format. The bacterial extract is either centrifuged at 12 000 g or 30 000 g, giving rise to a S12 and S30 extract respectively. The reaction occurs either in one compartment, in a batch-format (Fig. 10) or in two compartments, continuous-exchange format, where the reaction mixture is separated by a dialysis membrane from the feeding mixture, exchanging with the reaction mixture precursors and breakdown products (Schwarz et al., 2007). The continuous-exchange CFPE brings higher yield in terms of mg of protein per ml or reaction mixture, but is more demanding on precursor supply, e.g. amino acids. This can be a significant disadvantage for expression of isotope labeled proteins due to the high cost of isotope labeled amino acids, which exceed by far the cost of any other component.

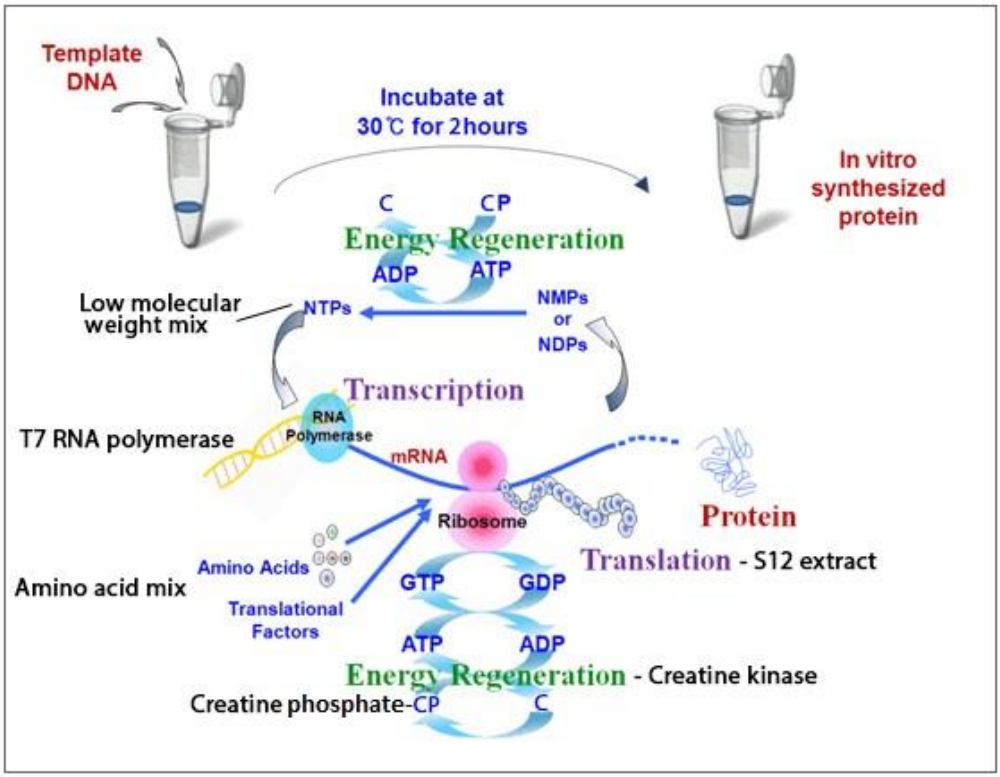

Fig. 10. Schematic depiction of a batch-format cell-free protein expression based on a bacterial S12 extract. The system is composed of a template DNA, a bacterial extract (contains the transcription and translation machinery), exogenously added amino acids, extra T7 RNA polymerase, a low molecular weight mix (a source of nucleotides, other additives and creatine phosphate as an energy regeneration source), creatine kinase and if needed a detergent is included. This picture is a modification of a picture published for the AccuRapid™ Cell-Free protein expression kit.

CFPE improved for a more effective expression of isotope labeled proteins

CFPE is also convenient for synthesis of proteins with isotope labeled amino acids, as the system is devoid of amino acids apart from those that are added exogenously. With the aim to increase amino acid incorporation and thereby achieve an economically sound in-house CFPE of isotope labeled proteins for NMR spectroscopy applications, Pedersen et al. (2011) investigated the optimal concentrations of key compounds of CFPE and the effect of different additives on expression yield, resulting in a modified protocol with a twofold to threefold enhanced yield. They confirmed the bacterial S12 extract is beneficial for the expression yield compared to the S30 extract and added one dialysis step to the extract preparation protocol in order to completely remove endogenous amino acids. Further, they optimized the amino acid concentrations (Gln, Ser), increased creatine phosphate content, and they added components of the citric acid cycle (malic acid, 2-oxoglutaric acid, succinic acid).

Site-specific incorporation of an unnatural amino acid into a polypeptide chain

There are various techniques for site-specific incorporation of unnatural amino acids (UAAs) into proteins based on removal of the *E.coli* release factor 1 (RF1), which binds to the stop codon UAG and triggers termination of translation. The site in the template DNA, which corresponds to the location where the UAA is to be incorporated into the polypeptide chain, is mutated so that the mRNA sequence is UAG. This is then recognized by the anticodon of a suppressor tRNA linked to the UAA by an aminoacyl tRNA synthetase. Conventional techniques do not always succeed in complete removal of the RF1 and they give strongly context dependent expression yields (depending for example on the incorporation site and the specific UAA) and face various difficulties with the incorporation of UAA in *in vivo* systems (reviewed in Loscha et al., 2012). With the goal to overcome these drawbacks, Loscha et al. (2012) developed a continuous-exchange cell-free system that allows facile, inexpensive, and complete removal of the release factor RF1 from a bacterial S30 extract derived from the widely used high-yielding and protease-deficient E. coli strain BL21 Star (DE3). The approach relies on replacing wild-type RF1 by a mutant with a C-terminal affinity tag consisting of three consecutive chitin-binding domains (RF1-CBD_3) for selective removal by filtration through a chitin column after production of an S30 extract in the usual way. The chitin-binding-domain tag allows the removal of RF1 under conditions that maintain the full activity of the S30 extract and at the same time delivers dramatically improved incorporation yields of difficult UAAs at difficult positions, suppresses the production of truncated protein, and allows the incorporation of UAAs at multiple sites in the same protein.

CFPE successfully used for expression of membrane proteins

The CFPE system can be very useful for membrane protein (MP) expression, as *in vivo* MP overexpression is often hampered by aggregation and cytotoxicity which can be consequences of saturation of the translocation or trafficking machinery used by cells to correctly insert the proteins into a membrane bilayer. The advantage of CFPE is that it facilitates co-translational solubilization of MPs in a wide range of detergents, lipids and nanodiscs (Isaksson et al., 2012). Beside few detergents not compatible with the CFPE, a variety of detergents can be used within a given concentration range, a compromise between maximal protein solubilization and minimal CFPE inhibition (Schwarz et al., 2007).

Isaksson et al. (2012) succeed in CFPE of 37 out of 38 MPs, both prokaryotic and eukaryotic, including human. All proteins except for control protein GFPcyc3 were insoluble and a suitable detergent had to be added. The most universal detergent turned out to be Brij®-58 (Polyoxyethylene (20) cetyl ether), followed by DDM (n-dodecyl-ß-D-maltoside), whereas some other detergents solubilized only a specific protein. When choosing a detergent, not only solubilization of the protein but also proper folding, functionality, downstream purification steps (e.g. tag cleavage), and subsequent structural analysis must be taken in account.

3 AIM OF THE PROJECT

I was trying to establish conditions for functional cell-free expression of the pore-only sodium channel Na_vSp1p for 2D IR studies. To achieve this I had to:

1. Prepare all components for cell-free protein expression (CFPE) and test their functionality by green fluorescent protein (GFP) expression
2. Establish cell-free expression of the Na_vSp1p
3. Purify the Na_vSp1p
4. Select sites within the channel that allow the study of ion selectivity by 2D IR studies and prepare mutated DNA

4 MATERIAL AND METHODS

Frequently used chemicals

Acetic acid (glacial) 100%, Merck KGaA; Ammonium hydroxide, ACS Reagent grade, ICN Biomedicals; Ampicillin sodium salt, ultrapure, USB Corporation; cOmplete EDTA-free, Roche Applied Science; Dithiothreitol (DTT) BioChemica, AppliChem; DNA Grade Agarose, Invitrogen™; EDTA, analytical reagent, VWR Prolabo; Glycerol, GPR Rectapur, 100%; HEPES (4-(2-Hydroxyethyl)piperazine-1-ethanesulfonic acid) for biochemistry, VMR Prolabo; Hydrochloric acid fuming 37% for analysis EMSURE® ACS, ISO, Reag. Ph Eur, Merck; Isopropyl-β-D-Thiogalactopyranoside (IPTG), Dioxane Free, Affymetrix; Kanamycin sulfate BioChemica, AppliChem; liquid nitrogen for flash freezing of samples; Magnesium acetate tetrahydrate, Sigma Aldrich, ≥ 99%; Magnesium chloride hexahydrate, AnalaR NORMAPUR, VMR Prolabo; β-mercaptoethanol VMR Prolabo; Methanol LiChrosolv, Merck KGaA, 99.8%; Ni-NTA Agarose, Qiagen; Phenylmethanesulfonylfluoride (PMSF), AppliChem, 99%; Potassium hydroxide pellets, Merck KGaA; Sodium chloride, GPR Rectapur, VWR Prolabo; Sodium hydroxide pellets, Merck KGaA, 99%; Sodium phosphate dibasic, Ph. Eur., Applichem Panreac; Sodium phosphate monobasic dihydrate, for analysis, Merck; Tris base (Tris(hydroxymethyl)aminomethane), for electrophoresis, VMR Prolabo; Yeast extract for microbiology, Fluka

Frequently used equipment and material:

Eppendorf Research® plus pipettes; Axygen Pipet tips; Accurpette pipette controller, VWR®; VWR® Disposable Serological Pipets, sterile, 10 ml; Microtubes 1.5 ml, tubes 15 ml and 50 ml from Sarstadt; Vivaspin ultrafiltration spin columns, Santorius; Spectra/Por 2 dialysis tubing, 12-14 kDa molecular weight cut off (MWCO), Spectrum Laboratories, Inc.;

Milli-Q Direct Water Purification System, Merck Millipore – produced water meets the specifications for EP and USP Purified water and was used for any experiment (mQ)

French Press Cell Disrupter, Thermo Spectronic,

Autoclaves: Systec HX 430, Systec DX 65

Shakers: Innova 43®, Eppendorf; benchtop shaker HT Infors Unitron; Eppendorf Thermomixer® C

Microcentrifuge: Centrifuge 5418 R and Centrifuge 5415 D, Eppendorf

Tabletop centrifuge: DR15 LabVision; 4-16KS, Sigma

Preparative centrifuge: Avanti J-25, J-26 XP; rotors JA 8.100 and JA-10, Beckman Coulter

Ultracentrifuge: Optima L-90K and LE-80K, rotors Ti 70 and Ti 45, Beckman Coulter

UV-VIS spectrophotometers: UV 1601 Shimadzu, NanoDrop 1000 (Thermo Scientific)

Fast protein liquid chromatography system: ÄKTAprime plus, ÄKTAexplorer, Unicorn software

Agilent Cary 630 FTIR spectrometer with Diamond ATR Accessory

Pymol, Adobe Photoshop

Cell Cultivation

Lysogeny Broth (LB medium) – 1% (w/v) peptone from casein, 0.5% (w/v) yeast extract, 1% (w/v) sodium chloride, pH 7.0; poured into Erlenmeyer flasks/ 50 ml tubes of the size of min. 5 x medium volume, autoclaved

2x YT Broth - 1.6% (w/v) peptone from casein, 1% (w/v) yeast extract, 0.5% (w/v) sodium chloride, pH 6.8-7.0; poured into Erlenmeyer flasks of the size of min. 5 x medium volume, autoclaved

Antibiotics (ATB) – ampicillin and kanamycin were kept as a 1000X stock solution (100 mg/ml), stored at -20ºC and added to the medium just prior to use at a final concentration 100 µg/ml unless stated otherwise

LB agarose plates – 1.5% (w/v) agarose was added to LB medium and autoclaved. Work environment was kept sterile (bunsen burner, 70% ethanol). Bottles were left to cool down to ~ 55°C and antibiotics were added as intended. A thin layer was poured into Petri plates (approximately 20 ml/ plate), covered with a lid, inverted when they had cooled down, and stored at 4°C. Prior to use, plates were warmed to 37°C.

Glycerol stock cultures of *E.coli* – a mini preculture (5 ml LB medium) supplemented with ATB was inoculated with a single colony from a freshly streaked agarose plate and grown over night (37°C, 220 rpm). Then 100 ml of LB medium with ATB was inoculated with 1 ml preculture and after 6 hours of growth (37 °C, 200 rpm), cells were harvested by centrifugation (5000 g, 20 min, 4°C). Cells were resuspended in 800 µl media and 800 µl sterile 85% glycerol, flash frozen and stored at - 80°C.

4.1 Origins of DNA constructs

Green fluorescent protein, cycle 3 mutant (GFPcyc3) cloned into pIVEX2.4d was a kind gift from Anders Pedersen (Isaksson et al., 2012) as well as the T7 RNA polymerase (T7) in pAR1219 (Davanloo et al., 1984). Daniel L. Minor (Shaya et al., 2011) kindly provided the human rhinovirus 3C protease (HRV 3C) cloned into pET28 and the pore domain construct of the voltage gated sodium channel (Na_vSp1p) in pHM3C vector, which was then cloned into pIVEX2.4d.

The constructs were transformed into One Shot® BL21 Star and except for T7 also into TOP10 Chemically Competent *E. coli* Cells (Invitrogen™) following manufacturer's instructions and a glycerol stock of each culture was prepared.

4.2 Cell-Free Protein Expression (CFPE)

The working environment was kept as RNAse-free as possible when performing CFPE experiments. A lab coat and gloves were worn at all times, bench surface, pipettes, electrodes and gloved hands were treated with an RNAse inhibitor (RNaseZAP®, Sigma). Work was carried out on an open bench under an open flame. Only certified RNAse-free plastic lab ware was used (Axygen Aerosol Barrier Filter Tips; Protein LoBind Tubes 1.5 ml, Eppendorf; 50 ml conical tubes, Greiner Bio- One). All solutions were prepared with RNAse-free mQ (preparation see 4.2.1).

The system for CFPE consists of the following components:

Component	**Stock solution**	**Final concentration**
RNAse-free water (DEPC- mQ)	-	-
DNA	-	0.01 µg/ µl
Magnesium acetate	500 mM	15-20 mM
Detergent in case of Na_vSp1p	20x	1x
Amino acid mix	5 mM	1 mM
Low molecular weight mix	5x	1x
L-Serine	168 mM	1 mM
L-Glutamine	168 mM	3 mM
T7 RNA polymerase	5 mg/ml	0.5 mg/ml
Creatine kinase	10 mg/ml	0.125 mg/ml
Bacterial S12 extract	-	31% (v/v)

All components were mixed in the listed order and incubated for 2 h at 30°C and 800 rpm.

4.2.1 RNAse-free ultrapure water (DEPC-mQ)

Diethylpyrocarbonate (DEPC, 1ml/l, BioChemica AppliChem) was added to mQ, incubated overnight at room temperature and autoclaved.

4.2.2 Detergents

The choice of detergents and their concentration was based on the review from Schwarz et al. (2007). Brij®-58 (Polyoxyethylene (20) cetyl ether) and Brij®-78 (Polyoxyethylene (18) octadecyl ether) from Sigma were used at a final concentration of 10 x critical micelle concentration (CMC), 0.8 mM and 0.46 mM respectively. DDM (n-dodecyl-ß-D-maltoside) and DM (n-Decyl-β-D-maltoside) from Anagrade Affymetrix were used at 3 x CMC, 0.6 mM and 5.4 mM respectively.

4.2.3 5 mM Amino acid mix (5 mM AA mix)

L-Isoleucine – Sigma, purity ≥ 98%
L- Leucine – Sigma, purity ≥ 98%
L-Lysine – Calbiochem, purity ≥ 99.7%
L-Methionine – Fluka, purity ≥ 99%
L-Phenylalanine – Sigma, purity ≥ 99%
L-Threonine – Sigma, purity ≥ 98%
L-Tryptophan – Sigma, purity ≥ 98%
L-Valine – Sigma, purity ≥ 98%
L-Arginine– Sigma, purity ≥ 98%
L-Histidine – Sigma, purity ≥ 99%
L-Alanine – Sigma, purity ≥ 99.5%
L-Asparagine – Sigma, purity ≥ 98%
L-Aspartate– Sigma, purity ≥ 98%
L-Cysteine – Aldrich, purity ≥ 97%
L-Glutamate – Sigma, purity ≥ 99%
L-Glutamine – Sigma, purity ≥ 99.5%
L-Glycine– Sigma, purity ≥ 98%
L-Proline – Merck KGaA, for biochemistry
L-Serine – Sigma, purity ≥ 99%
L-Tyrosine – Sigma, purity ≥ 98%

A 5 mM stock solution was prepared by mixing equal amounts of 100 mM solutions of each amino acid. To obtain the amino acid solutions, all amino acids except tryptophan and tyrosine were dissolved in 60 mM HEPES-KOH, pH 7.5. Tryptophan and tyrosine were dissolved in 0.7 M hydrochloride acid and 0.7 M potassium hydroxide respectively. Methionine and cysteine solutions were supplemented with DTT to a final concentration of 4 mM and 8 mM respectively. Solutions were stored at - 20°C.

4.2.4 5x Low molecular weight mix (5x LMW mix)

First, a buffering solution was prepared from the following salts:

Buffer	**5x concentration**
Ammonium hydroxide	137.2 mM
D-Glutamic acid, Sigma, purity ≥ 99%	1.06 M
5 M potassium hydroxide	1.15 M
1 M Hepes-KOH, pH 7.0	262.5 mM

The pH was adjusted using acetic acid or potassium hydroxide and only then following compounds were added:

Compound	**5x concentration**
Adenosine 5′-triphosphate disodium salt hydrate, Aldrich, 99%	5.5 mM
Guanosine 5′-triphosphate sodium salt hydrate, Sigma, ≥ 95%	4 mM
Cytidine 5′-triphosphate disodium salt, Sigma, ≥ 95%	4 mM
Uridine 5′-triphosphate trisodium salt dihydrate, Sigma, ≥ 80%	4 mM
Adenosine 3′,5′-cyclic monophosphate, Sigma, ≥ 98.5%	3.2 mM
Folinic acid calcium salt hydrate, BioXtra, ≥ 99%	0.34 mM
DTT	8.5 mM
Creatine phosphate, Roche Applied Science, > 97% Creatine phosphate disodium salt tetrahydrate	0.315 M
L-(-)-Malic acid; Fluka, ≥ 99%	22 mM
Disodium succinate hexahydrate, SAFC, ≥ 98%	7.5 mM
α-Ketoglutaric acid, Fluka, ≥ 99.0%	9,5 mM
tRNA, Roche Applied Science	0.875 mg/ml
RiboLock RNase Inhibitor, Thermo Scientific	40 U/ml
cOmplete EDTA-free, Roche Applied Sciences	1 tablet per 10 ml

The pH was again adjusted to 7.0 and aliquots were flash frozen and stored at -20°C.

4.2.5 L-Serine

L-serine was dissolved in 60 mM HEPES-KOH (pH 7.5) to obtain a 168 mM stock solution.

4.2.6 L-Glutamine

L-glutamine was dissolved in 60 mM HEPES-KOH (pH 7.5) to obtain a 168 mM stock solution.

4.2.7 T7 RNA Polymerase (T7) expression and purification

The plasmid encoding T7 contained an ampicillin resistance gene and a *lac* operon, which was induced by adding isopropyl β-D-1-thiogalactopyranoside (IPTG, inactivates the *lac* repressor), and started the expression of T7 in the exponential growth phase of the *E.coli* cells. The purification comprised two steps, ammonium sulfate precipitation and ion-exchange chromatography. Ammonium sulfate precipitation is based on altering of the ionic strength leading to a reversible precipitation of the protein. In ion-exchange chromatography, proteins bind to the column depending on their net charge (depends on the pH) and are eluted by increasing the ionic strength of the mobile phase.

Buffer A	Buffer B	Buffer C
50 mM Tris-HCl, pH 8.1	20 mM NaPi, pH 7.7	20 mM NaPi, pH 7.7
20 mM NaCl	1 mM EDTA	1 mM EDTA
2 mM EDTA	1 mM DTT*	1 mM DTT*
1 mM DTT*	1 mM PMSF*	5% v/v glycerol
1 mM PMSF*	5% v/v glycerol	

*due to instability, these components were added just prior to usage. PMSF was diluted from a 0.6 M methanol stock solution.

As preculture, 100 ml LB medium supplemented with ampicillin was inoculated with a freeze culture of *E. coli* BL21 (DE3)-Rosetta cells transformed with pAR1219 (Davanloo et al., 1984) and grown overnight at 37°C and 200 rpm. Next morning, 2 liters LB medium with ampicillin was inoculated with 20 ml preculture and grown at 37°C, 175 rpm till OD_{600} reached 1. Protein expression was induced by adding 0.8 mM (IPTG). After six hours, cells were harvested by centrifugation (JA 10, 5000 g, 15 min, 4°C) and resuspended in 45 ml of buffer A containing 1 tablet of cOmplete EDTA-free. Cells were flash frozen and allowed to thaw at 8°C overnight. Next day, cells were disrupted by a French press, using two passages at 24 000 psi. After the first passage, a spatula tip of DNase I and a little of buffer A containing 1 tablet of cOmplete EDTA-free was added to the cell lysate. Then the cell lysate in a 50 ml plastic tube was

immersed in ice water and sonicated at 60 W using 4+4 s pulses for less than 1 minute (Q700 Sonica). Afterwards, cell debris was separated from the lysate be ultracentrifugation (Ti 70, 45 000 g, 1 h, 4°C). Supernatant was transferred into an Erlenmeyer flask, 10 ml of 2 M ammonium sulfate (Merck KGaA, 99.5%) was added and the volume was adjusted to 110 ml with buffer A containing 2 tablets of cOmplete EDTA-free. Slowly 0.82 volumes (90.2 ml) chilled, saturated ammonium sulfate solution, pH 7 adjusted with Tris powder, was added to the supernate while it was stirred. The solution was left to stir at 8°C for at least 15 minutes and then ultracentrifuged (Ti 45, 12 000 g, 15 min, 4°C). The supernatant was discarded and the pellet was resuspended in 90 ml buffer B containing 100 mM sodium chloride and 2 tablets of cOmplete EDTA-free and dialyzed against 8 l buffer B containing additional 100 mM sodium chloride (MWCO 12-14 kDa, 4 h, 8°C). Dialysis was repeated overnight against 8 l of buffer B containing 35 mM NaCl. On the next morning, the sample was centrifuged for 10 min at 4 000 g before sterile filtering the sample through a 0.22 µm filter. Sample was diluted 1:1 with buffer C and loaded onto a Q Sepharose Fast Flow column (GE Healthcare) that had been equilibrated with buffer C containing 20 mM NaCl. The column was washed with at least one column volume of buffer C containing 20 mM NaCl before eluting the protein with a 250 ml gradient between 20 mM and 1 M NaCl, using buffer C. Eluted sample was concentrated to 15 mg/ml and mixed with an equal amount of sterile glycerol. The concentration was determined using an extinction coefficient of 140 000 M^{-1} cm^{-1} at 280 nm. Aliquots were flash frozen and stored at -20°C.

4.2.8 Creatine kinase

Lyophilized creatine kinase from rabbit muscle was purchased from Roche Applied Science. The lyophilisate was dissolved in RNAse-free mQ to 10 mg/ml and aliquots were flash frozen and stored at -20°C.

4.2.9 Bacterial S12 extract

4.2.9.1 Cell cultivation

In the evening, 100 ml 2xYT Broth, pH 6.8 containing kanamycin were inoculated with a glycerol freeze culture of genomically modified *Escherichia coli* BL21 (DE3)::RFI-CBD_3 (Loscha et al., 2012). This preculture was grown overnight in a shaking incubator at 37°C at 200 rpm. Next morning, 2x 100 ml 2xYT were

inoculated with 1 ml preculture each. After four hours of growth, a 20 l fermenter (Biostat C, B. Braun Biotech International) already prepared according to Table 1 and filled to a total volume of 20 l was inoculated with both cultures.

Table 1. Preparation of the 20 liter fermenter

2xYTPG:	320 g tryptone (peptone from casein) 200 g yeast extract 100 g sodium chloride 8 ml 1 M sodium hydroxide 68,64 g sodium phosphate monobasic dihydrate (22 mM) 131,6 g sodium phosphate dibasic (40 mM)

2xYTPG solutes were dissolved in 17 l water within the fermenter and 15 ml Antifoam C Emulsion (Sigma) was added.

After sterilization of the media following manufacturer's instructions, 1 l of sterile 20% (w/v) glucose monohydrate solution and the following compounds (p-aminobenzoic acid was dissolved in 5 ml of DMSO, Sigma-Aldrich, ≥ 99.9%) were added and the volume adjusted to 20 l using sterile mQ water:

Compound:	mg/l	mg/ 20 l:
Choline chloride, Fluka Analytical, ≥ 97%	28.6	572
Nicotinic acid (Niacin, Vitamin B_3), Acros, ≥ 99.5%	25.1	502
p-Aminobenzoic acid, Aldrich, 99%	20.0	400
Pantothenic acid calcium salt (Vitamin B_5), Fluka, 99%	9.4	188
Pyridoxal-5-phosphate (Vitamin B_6), Sigma, ≥ 98%	1.8	36
(-)-Riboflavin (Vitamin B_2), Sigma, ≥ 98%	3.9	78
Thiamine hydrochloride (Vitamin B_1), USB Corporation	17.7	354
Betaine hydrochlorid, Calbiochem, 99.5%	33.1	662
D-Biotin, MP Biomedicals	0.1	2
Cyanocobalamin (Vitamin B_{12})	0.01	0.2
Folinic acid calcium salt hydrate, BioXtra, ≥ 99%	0.075	1.5
Iron (III) chloride hexahydrate, Scharlau Chemie S.A., 99%	20	400
Sodium molybdate dehydrate, Acros, ≥ 99%	3.5	70
Boric acid, Sigma, ≥ 99.5%	1.2	24
Cobalt sulphate heptahydrate, Sigma, ≥ 99%	4	80
Copper sulphate pentahydrate, Merck KGaA, 99%	3.4	68
Mangan suplhate hydrate, pro analysi, Merck	1.9	38

Zinc sulphate heptahydrate, Scharlau Chemie S.A., 99.5%	3.4	68
Amino acids (for suppliers and purity see 4.1.2 5 mM Amino acid mix)		
L-Aspartate	28.5	570
L-Glycine	49.1	982
L-Histidine	9.35	187
L-Isoleucine	26.2	524
L-Leucine	29.9	598
L-Lysine	31.4	628
L-Methionine	14.9	298
L-Phenylalanine	15.3	306
L-Proline	31.8	636
L-Threonine	37.7	754
L-Tryptophan	102.1	2 042
L-Tyrosine	37.7	312
L-Valine	117.1	2 342

After inoculation, the culture was grown at 37°C with 600-800 rpm stirring. The pH 7 was controlled with a 2 M sodium hydroxide solution (almost 500 ml needed) and the air flow was set at 8 l/min. When OD_{600} reached 4.5, the temperature was decreased to 10°C, and the cells were transferred into chilled JA 8.1000 centrifuge bottles by passing them through a stainless steel coil immersed in ice water. The cell suspension was harvested by centrifugation (4000 g, 15 min, 4°C), the supernatant was discarded, and the cells were washed by resuspending them in 3 l of chilled extract buffer (composition see below), pelleted again, and resuspended in 10 ml extract buffer/ 8 g of wet cells. Extract buffer was supplemented with 1 tablet cOmplete EDTA-free per 50 ml cell suspension. Cells were flash frozen and kept at - 80°C until the next preparation step.

4.2.9.2 Bacterial S12 extract preparation

Extract buffer

10 mM Tris-acetate, pH 8.2 (Trizma® acetate, Reagent grade, Sigma)

14 mM magnesium acetate tetrahydrate

60 mM potassium acetate, Merck KGaA, extrapure

Cells were disrupted by a French press using two passages at 24 000 psi. Cell lysate was centrifuged at 12 100 g for 10 minutes. The supernatant was decanted into RNAse-free tubes and divided into two parts in order to produce one extract with the chitin binding domain tagged release factor 1 (w CBD-RFI) and one without (w/o CBD-RFI). Both were incubated for 120 min at 30°C, 150 rpm. One part (w) of the supernatant was supplemented with DTT to a final concentration of 1 mM and dialyzed twice against 4 l of extract buffer, which was just prior to use supplemented with the protease inhibitor β-mercaptoethanol (1 ml/ l). The other part (w/o) was handled in the same manner, except that after incubation, the extract was first loaded onto 20 ml chitin resin (New England Biolabs) equilibrated with extract buffer and only the flow-through was supplemented with DTT and first dialyzed against 3 l of 33% PEG 8000 in extract buffer prior to the two dialysis steps. Single-use aliquots were flash frozen and stored at - 80°C.

4.2.10 DNA purification and restriction-enzyme analysis

DNA purification from TOP10 *E.coli* cells was done following the high-copy plasmid high yield protocol from the Qiagen Plasmid *Plus* Midi/Maxi Kit except that DNA for cell-free protein expression was eluted with RNAse-free mQ water. Concentration was determined by absorbance at 260 nm using the NanoDrop. DNA purification was followed by a restriction endonuclease digestion and staining. GFPcyc3 plasmid was digested by Bam HI, Xba I, Na_vSp1p by Xba I, Sal I and 3C HRV by Sma I, Sac I and, additionally, by Sma I, Xba I (all Thermo Scientific).

Sample preparation: 0.3-0.5 µg DNA, 1.5 µl 10X FastDigest Green Buffer (Thermo Scientific), 0.7 µl of each enzyme, adjusted with mQ to 15 µl.

Ladder preparation: 2 µl 1 kb Plus DNA Ladder (Invitrogen™), 2 µl 10X FastDigest Green Buffer, 16 µl mQ

Samples were incubated at 37 °C for 15 min and then samples and ladder were loaded onto a 0.7% agarose gel in 0.5 X TAE buffer (20 mM Tris, 10 mM acetic acid, 0.5 mM EDTA, pH 8), 10 µl/ well.

Electrophoresis was performed at 135 V for 22 min in a Mupid-exU system (Advance). Gel was stained with 5 µl of SYBR® Safe DNA Gel Stain (life technologies) in 50 µl 0.5 X TAE buffer for 30 min on a shaker. DNA fragments were detected at 365 nm with AplhaImager® HP System, Aplha Innotech.

4.3 GFPcyc3 expression and purification

The plasmid encoding GFPcyc3 contained an ampicillin resistance gene and the *lac* operon was induced by IPTG to start expression of GFPcyc3 in the exponential growth phase of the *E.coli* cells.

The polyhistidine-tagged protein was purified by gravity-flow immobilized metal ion affinity chromatography (IMAC). Nickel ions immobilized by a modified nitrilotriacetic acid (Ni-NTA) to a solid support bind with covalent bonds the His-tagged protein in the mixture and the protein is subsequently eluted with a higher concentration of imidazole, which has a greater affinity to the nickel ions than the His-tagged protein. Fig. 11 shows the general steps of a Ni-NTA purification.

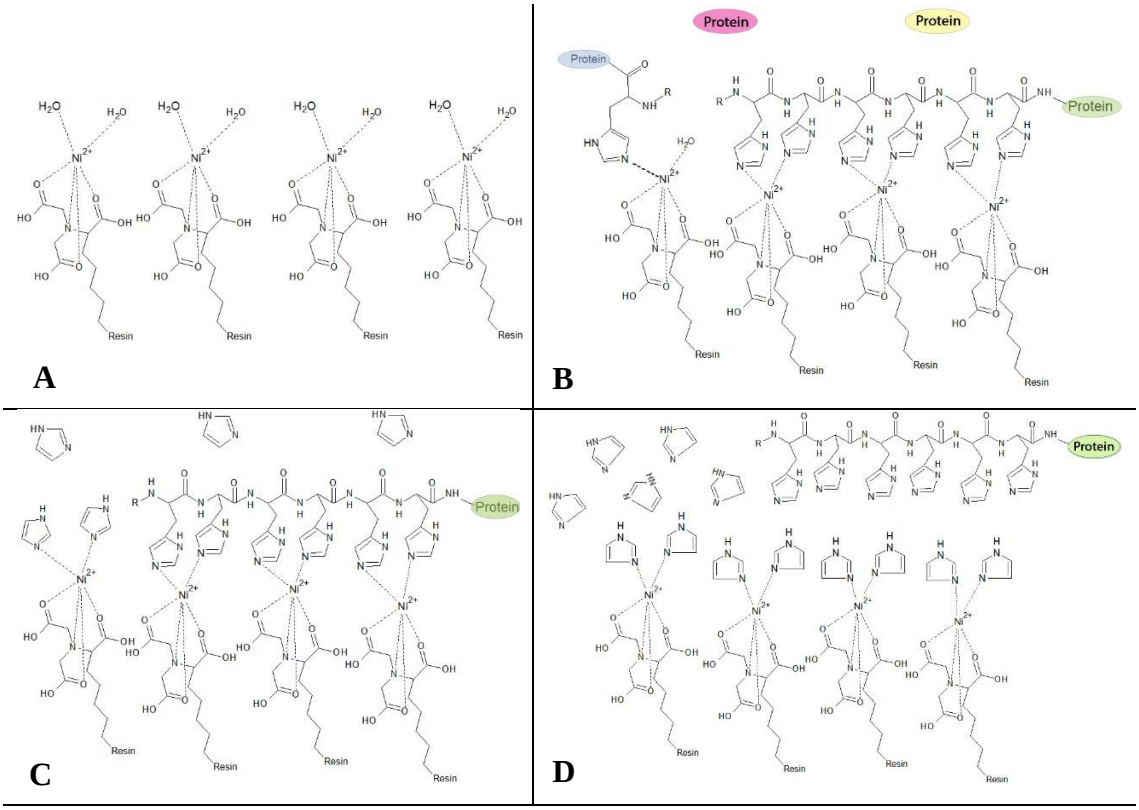

Fig. 11. Protein purification steps on a Ni-NTA column. (*A*) Modified nitrilotriacetic acid immobilizes Ni^{+} to a solid support (agarose). (*B*) The sample is loaded onto the column. The tagged protein binds to the column (green protein), but also other proteins bind to the column with their histidines (blue protein). (*C*) The column is washed with a low imidazole concentration to eliminate non-specific binding. (*D*) The His-tagged protein is eluted with a high imidazole concentration.

In the morning, a start culture of 50 ml LB medium supplemented with 2X AMP was inoculated from a glycerol freeze culture of *E.Coli* BL21 Star (DE3) transformed with pIVEX2.4 encoding a His-tagged GFPcyc3, and grown at 200 rpm, 37°C. In the evening, 50 ml overnight culture (LB, 2X AMP) was inoculated with 500 µl of preculture and grown overnight (200 rpm, 37°C). Next morning, 4 x 500 ml LB medium

(2X AMP) was inoculated with 5 ml overnight culture, grown for one hour at 37°C and then the temperature was decreased to 30°C. When $O.D._{600}$ reached 0.6, expression was induced by adding 1 mM IPTG. After three hours, cells were harvested by centrifugation (JA-10, 6000 g, 20 min, 4°C) and the cell pellet was resuspended in 40 ml lysis buffer (25 mM Tris-HCl, 250 mM NaCl, pH 8) supplemented with 1 tablet cOmplete EDTA-free. Cells were flash frozen and stored at 8°C overnight. Lysis was performed by ultrasound and cell lysate was separated from unbroken cells and cell debris by centrifugation (Ti 70, 45 000 g, 1 h, 4°C). Supernatant was incubated for 15 min at 4°C with 2 mM magnesium chloride and a little DNase I (AppliChem). To purify the protein by affinity chromatography, supernatant was supplemented with 10 mM imidazole and loaded onto a 2 ml Ni-NTA agarose column equilibrated with loading buffer (lysis buffer with 10 mM imidazole). The column was washed with 20 ml loading buffer followed by a second wash of 7 ml lysis buffer supplemented with 50 mM imidazole. The first GFPcyc3 fraction was eluted with 5 ml elution buffer (lysis buffer with 150 mM imidazole). Second fraction was eluted after the column was incubated with additional 3 ml elution buffer for 30 min and final elution was performed with 4 ml of lysis buffer with 200 mM imidazole. Eluted fractions were dialyzed overnight against 5 l lysis buffer (MWCO 12-14 kDa). Concentration was determined photometrically using a NanoDrop. The extinction coefficient of GFPcyc3 is 22 015 M^{-1} cm^{-1} and the M.W. is 29.81 kDa. Protein was flash frozen and kept at -80°C. Purity was verified by SDS-PAGE analysis.

4.4 Purification of the pore-only sodium channel (Na_vSp1p)

Purification was based on immobilized metal ion affinity chromatography (principle Fig. 11.) as the vector harbors an N-Terminal 6x His-tag together with a maltose binding protein (MBP) and a HRV 3C protease cleavage site. MBP is a highly soluble protein used as a fusion partner for insoluble proteins to enhance their proper folding (Kapust & Waugh, 1999). Aligned from the N- to C-terminus, the HRV 3C protease cleavage site follows after the N-Terminal 6x His-tag and the MBP (Fig. 12). HRV 3C is a highly specific protease from *Human rhinovirus* with the recognition cleavage sequence Leu-Glu-Val-Phe-Gly-Pro. The protease also contained a His-tag for convenient removal after cleavage.

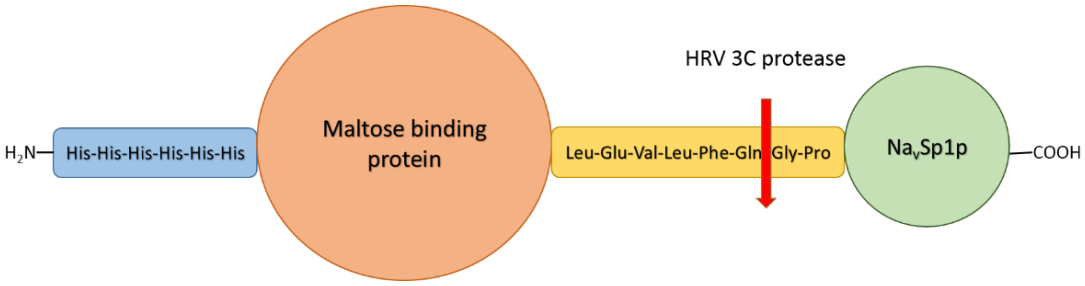

Fig. 12. Schematic depiction of the fusion protein containing Na_vSp1p. The red arrow marks the cleavage by 3C HRV protease in the cleavage site (yellow).

The final purification step was gel filtration chromatography (a type of size-exclusion chromatography, SEC), a method separating macromolecules by their size as they move through a bed of porous beads and the smaller the molecule, the more it diffuses into the beads, resulting in a bigger elution volume.

The purification protocol we used was a modification of the protocol published by Shaya et al. (2011).

Buffer A	Buffer C
20 mM Tris pH 8.0	20 mM Hepes pH 8.0
200 mM NaCl	200 mM NaCl
8% (vol/vol) glycerol	2.7 mM DM
2.7 mM DM	

Completed CFPE reaction was centrifuged (Ti 45, 13 600 rpm, 20 min, 4°C) and the supernatant was loaded onto a gravity flow Ni-NTA agarose column (I. Ni-NTA) equilibrated with 10 CVs of buffer A. The column was washed with 7 CVs buffer A supplemented with 20 mM imidazole. Protein was eluted by step application of buffer A supplemented with 300 mM imidazole over 3 CVs. Eluted protein was desalted using

either a HiPrep Desalting column (GE Healthcare) or by dialyses (twice, against buffer A, volume 100-200 times sample volume, tubing MWCO 12-14 kDa). The affinity tag and the maltose binding domain of the protein were removed by adding a His-tagged 3C HRV Protease (Pierce, Thermo Scientific) at a ratio protein: protease = 10 mg: 1 mg at 8°C overnight with gentle agitation. Cleaved protein was separated from the uncleaved protein and protease by loading the reaction mixture onto a Ni-NTA agarose column (II. Ni-NTA) and colleting the flow-through and an additional wash with 2 CVs buffer A. Cleaved protein was concentrated to less than 500 µl prior to loading onto a Superdex 200 Increase 10/300 column (GE Healthcare) equilibrated with buffer C. Protein concentration was determined with NanoDrop, using an extinction coefficient for the uncleaved and cleaved protein of 90 300 M^{-1} cm^{-1} and 23 500 M^{-1} cm^{-1} at 280 nm respectively. Samples of each step were collected for SDS-PAGE analysis and the gel was blotted with a One Hour Western Blot Kit (details see 4.7.3).

4.5 HRV 3C protease expression and purification

The plasmid encoding HRV 3C protease harbored a kanamycin resistance gene and the *lac* operon was induced by IPTG to start expression of HRV 3C in the exponential growth phase of the *E.coli* cells. The protein was expressed with an octa-His-tag and purification was performed on a Ni-NTA column followed by dialysis, as imidazole inhibits the activity of the protease. Moreover, high concentrations of imidazole (300 mM) lead to complete protein precipitation, which can be largely avoided by using 150 mM imidazole.

Chelating buffer	Elution buffer	Dialysis buffer
50 mM Tris-HCl pH 8.0	50 mM Tris-HCl pH 8.0	50 mM Tris-HCl pH 8.0
300 mM NaCl	300 mM NaCl	150 mM NaCl
20 mM imidazole	150 mM imidazole	10 mM EDTA
10% glycerol	10% glycerol	20% glycerol
		5 mM DTT

As a preculture, 10 ml 2YT (pH 7) containing kanamycin was inoculated with a glycerol stock of pET28 in *E.Coli* BL21 Star and grown overnight (220 rpm, 37°C). Two liter cultures were inoculated with 6 ml of preculture and grown (180 rpm, 37°C) to an $O.D_{600}$ of 0.6-0.8. Then the temperature was reduced to 22°C and after 15 min, expression was induced with 0.4 mM IPTG. After 19 h cells were harvested by

centrifugation (JA 10, 6000 g, 20 min, 4°C). Pelleted cells were resuspended in 50 ml lysis buffer (chelating buffer with 1 mg lysozyme from chicken egg white, Sigma and 1 mM PMSF) and disrupted using French Press, two passages at 24 000 psi. Cell lysate was separated from unbroken cells and cell debris by ultracentrifugation (Ti 70, 42 000 g, 1 h, 4°C). The supernatant containing the octa-histidine tagged 3C protease was loaded onto a 5 ml HisTrap™ HP column (GE Healthcare) equilibrated with chelating buffer. Column was washed with chelating buffer containing 46 mM imidazole (80% chelating buffer and 20% elution buffer) until no more protein eluted. The bound protein was eluted by step application of elution buffer. Fractions containing the protein were collected and dialyzed overnight against 2 l dialysis buffer (MWCO 12-14 kDa, 8°C). The concentration was measured photometrically with an extinction coefficient of 5960 M^{-1} cm^{-1} at 280 nm and M.W. was 21.282 kDa. Aliquots (9.13 mg/ml) were flash frozen and stored at -20°C.

4.5.1 Functionality assay

To test the functionality of the protein, it was incubated with the positive control GST-Syk protein in the 10X cleavage buffer (500 mM Tris, 1.5 M NaCl, pH 7.5; both from the Pierce HRV 3C kit) at various protease: protein ratios and compared to the standard ratio 1:5 of the Pierce HRV 3C protease (Table 2). Incubation was carried out for 19 h at 8°C with gentle agitation. Cleavage efficiency was analyzed by SDS-PAGE and detected by staining with InVision™ His-tag In-gel Stain and Coomassie.

Table 2. Composition of samples for estimation of in-house purified HRV 3C functionality

			In-house purified 3C HRV (429 µM)				**Pierce 3C HRV (21 µM)**
protease: protein (mol/mol)	1:4.3	1:0.43	1:0.22	1:0.043	1:0.011	1:0.0043	1:4.4
10x cleavage buffer	2.5 µl						
3C HRV (nmol)	0.022	0.22	0.43	2.2	4.3	4.3	0.021
GST-Syk protein (18.52 µM) (nmol)	0.093	0.093	0.093	0.093	0.046	0.019	0.093
mQ	to 25 µl						

4.6 Mutation of Na_vSp1p

Three mutants with a single amino acid change were prepared following the QuickChange® Site-Directed Mutagenesis Kit (Stratagene) using 50 ng dsDNA template and the T3 Thermocycler, Biometra. Sequences of G181, L175 and S177 were changed to TAG, which encodes the mRNA stop codon UAG recognized by release factor 1 (RFI). Primers obtained from Eurofins MWG Operon had the following sequences (5`→3`):

Mutation of G181: GGAAAGCTGGTCGATG**tag**ATCGTTCGCCCGG

Reverse primer: CCGGGCGAACGAT**cta**CATCGACCAGCTTTCC

Mutation of L175: CGCTGTTCCAGATCATGACG**taG**GAAAGCTGGTCGATGG

Reverse primer: CCATCGACCAGCTTTC**Cta**CGTCATGATCTGGAACAGCG

Mutation of S177: CCAGATCATGACGCTGGAA**tag**TGGTCGATGGG

Reverse primer: CCCATCGACCA**cta**TTCCAGCGTCATGATCTGG

The 1st segment of the thermal cycling (Table 3) is heat activation of *PfuTurbo* ®DNA polymerase and it is the 2nd segment where the mutation during the polymerase chain reaction (PCR) occurs. In the first step of this repeated segment, template DNA melts, then at 55°C both primers anneal to single stranded DNAs and subsequently the polymerase binds to the primer-template hybrid and elongation (5`→3`) takes place.

Table 3.Thermal cycling for NavSp1p in pIVEX2.4d

Thermal cycling	**No. of cycles**	**Temperature**	**time**
1. segment	1	95°C	30 s
2. segment	16	95°C	30 s
		55°C	60 s
		68°C	5.27 min

To remove template DNA from the PCR product, it is then treated with *Dpn I*, an endonuclease digesting methylated and hemimethylated DNA, and leaving the mutation-containing synthesized DNA in the product (Fig. 13).

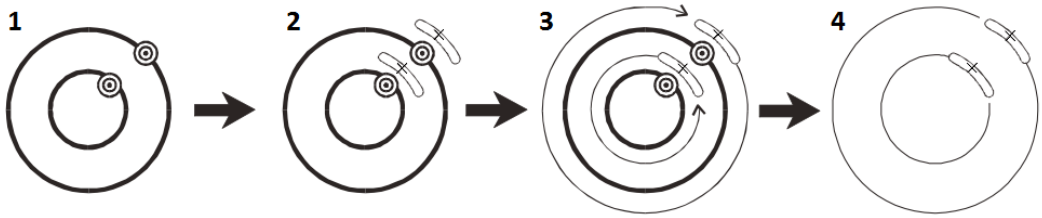

Fig. 13. Overview of the QuikChange® site-directed mutagenesis method. (*1*) Gene in plasmid with target site mutation. (*2*) DNA template melts and primers with desired mutation anneal. (*3*) Elongation and incorporation of the primers resulting in mutated circular strands. (*4*) DNA template was digested by *Dpn I* and the PCR product contains the circular, mutated dsDNA. Adapted from the QuikChange® Site-Directed Mutagenesis Kit, Instruction Manual, 2013.

Positive clones were confirmed by sequencing (Eurofins MWG Operon). Mutated DNA was transformed into One Shot®TOP10 Chemically Competent *E.coli* Cells (Invitrogen) and kept as a glycerol stock culture. DNA was purified and digested in the same manner as for Na_vSp1p (4.2.10).

4.7 Protein detection methods

4.7.1 GFPcyc3 fluorescence detection

GFP, green fluorescent protein, is a protein first discovered in *Aequorea* jellyfish exhibiting bright green fluorescence when exposed to light in the blue to UV range. GFPcyc3 is a GFP mutant with three point mutations causing a stronger fluorescence, a better expression profile in *E.coli* and a fast maturation within 3-4h compared to the overnight maturation of wild type GFP (Crameri et al., 1996).

After completed CFPE of GFPcyc3, the protein was incubated at 4°C for 3-4 h to maturate. Then it was centrifuged (13 600 rpm, 20 min, 4°C) and supernatant was pipetted into a black Nunc® MicroWell™ 96 well polypropylene plate (180 µl/ well). For fluorescence detection, the plate reader and software FLUOstar OPTIMA, LabVision was used, the excitation wavelength was 390 nm and emission was detected at 520 nm.

To determine GFPcyc3 concentration, GFPcyc3 obtained from bacterial cultivation (see 4.3) was used to prepare a series of standard solutions of known GFPcyc3 concentrations (0.1 µM, 0.3 µM, 1 µM, 3 µM, 5 µM GFPcyc3 in 25 mM Tris, 250 mM NaCl, pH 8).

4.7.2 SDS-PAGE

SDS-PAGE, sodium dodecyl sulfate polyacrylamide gel electrophoresis, is a method for separating proteins by their molecular weight under denaturing conditions. SDS is an anionic detergent that linearizes the proteins and imparts an even distribution of negative charge per unit mass. Therefore during electrophoresis, the negatively charged proteins migrating towards the anode will be separated solely by their size.

Protein expression and purification was analyzed by SDS-PAGE. Samples were supplemented with NuPAGE® LDS Sample Buffer (4X) (Novex®, life technologies) 3:1, heated for 10 minutes at 97°C and then along with 2 µl PageRuler Plus Prestained Protein Ladder (Thermo Scientific) and 6 µl of 6x His Protein Ladder (Qiagen) loaded into the wells of a NuPAGE® Novex® 4-12% Bis-Tris Gel in a XCell SureLock™ Mini-Cell (life technologies). Electrophoresis was performed in a MES Running buffer (for a 20X stock solution: 50 mM 2-(*N*-morpholino)ethanesulfonic acid (MES), 50 mM Tris base, 0.1% SDS, 1 mM EDTA, pH 7.3) at 200 V for 35 min.

Preparation of the 6x His Protein Ladder: The lyophilisate was dissolved in 62.5 µl of NuPAGE® LDS Sample Buffer (4X), 12.5 µl 1 M DTT and 175 µl mQ. Aliquots were flash frozen, stored at – 20°C and heated to 97°C for 10 min prior to usage.

4.7.3 Western blotting

Western blotting, or immunoblotting, is an analytical technique for detection of a specific protein in a mixture, based on an antigen-antibody reaction. Typically, the antibody carries a chemiluminescent marker, which enables the detection of the specific protein in the mixture.

The transfer of protein from a polyacrylamide gel to a nitrocellulose membrane was done following the manual for XCell II™ Blot Module in transfer buffer (25 mM Tris, 192 mM glycine, 20% methanol) at 30 V for 60 minutes. The Western blot was detected using ONE-HOUR Western™ Basic Kit (Mouse) (GenScript) according to manufacturer's instructions. Mixture I was prepared by mixing 5 µl Anti-His Antibody (GE Healthcare) with 80 µl of WB-1. Chemiluminescence was detected using hardware and software of Fujifilm Las-1000 Luminescent Image Analyzer Chemi Fuji.

4.7.4 InVision™ His-tag In-gel Stain

InVision™ His-tag In-gel Stain contains a proprietary fluorescent dye conjugated to a Ni^{2+}: nitrilotriacetic acid complex that binds specifically to the oligohistidine domain of the His-tagged fusion protein allowing specific detection of His-tagged fusion proteins from a mixture of endogenous proteins (InVision™ His-tag In-gel Stain, User Guide).

The staining of a NuPage® Novex Gel was performed following manufacturer's instructions (microwave procedure, 1 mm gel). For visualization and imagining at 302 nm, hardware and software of AplhaImager® HP System, Aplha Innotech was used.

4.7.5 Coomassie Brilliant Blue G-250 staining

Coomassie Brilliant Blue G-250 is a triphenylmethane dye for visualization of protein bands on polyacrylamide gels.

Coomassie Brilliant Blue G-250 staining (SimplyBlue™ SafeStain, life technologies) of a NuPage® Novex Gel was performed following manufacturer's instructions (microwave procedure, detection limit 5 ng bovine serum albumin).

5 RESULTS

We prepared all necessary components for CFPE and verified the functionality by GFPcyc3 expression. To quantify the amount of expressed protein, we used heterologously expressed and purified GFPcyc3 as a standard. Based on the observation that membrane proteins have been successfully expressed in a cell-free system (Isaksson et al., 2012) and that *E. coli* is a suitable host for expressing Na_vSp1p (Shaya et al., 2011), we tested the expression of Na_vSp1p in a cell-free system derived from a bacterial extract S12 from *E. coli*. First, the expression of the His-tagged Na_vSp1p was verified by immunoblotting in the crude expression mixture using anti-His antibodies. Second, a purification protocol was adapted based on the methods described by Shaya et al. (2011). To keep costs for production of mg amounts of NavSp1p reasonable, it was necessary to establish an in-house production of the HRV 3C protease. A preliminary FTIR spectrum of purified Na_vSp1p was recorded which corresponds to the alpha-helical structure of Na_vSp1p. Finally, three single amino acids within the selectivity filter of Na_vSp1p were mutated in order to be able to introduce isotope labeled amino acids in the future.

5.1 DNA preparation and restriction-enzyme analysis

DNA preparation and restriction-enzyme analysis was performed as described in 4.2.10. Preparation of GFPcyc3 DNA from 35 ml overnight (ON) culture resulted in 0.8 µg DNA, 100 ml of Na_vSp1p ON culture yielded up to 5.3 µg DNA and a 35 ml ON culture of 3C HRV yielded 0.3 µg DNA material. A restriction analysis was performed after each DNA purification in order to verify identity. Expected fragment sizes of Na_vSp1p were 1745 bp and 3527 bp, and 632 bp and 3610 bp for GFPcyc3. 3C HRV protease digestion with Sma I and Sac I was to produce 1259 bp and 4590 bp fragments and for Sma I and Xba I, 3965 bp and 1884 bp fragments were calculated. The sizes of detected fragments shown in Fig. 14*A*,*B* were in line with expected sizes and indicated that correct DNA was used each time.

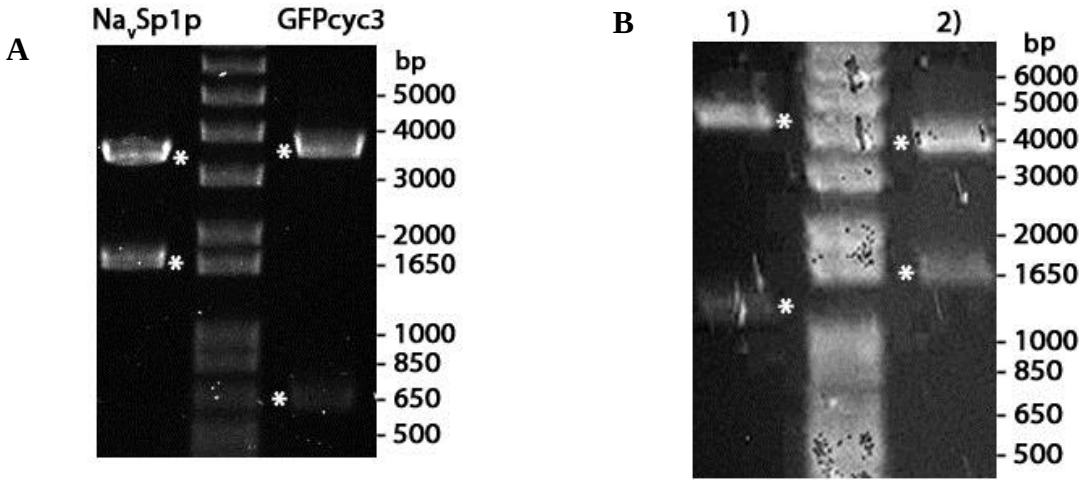

Fig. 14. DNA Restriction analysis of (A) NavSp1p (1745 bp, 3527 bp), GFPcyc3 (632 bp, 3610 bp) and (B) 3C HRV with 1) Sma I, Sac I (1259 bp, 4590 bp) and 2) Sma I, Xba I (3965 bp, 1884 bp). Fragments are marked with an asterisk.

5.2 CFPE components

All components except the creatine kinase needed to be newly prepared and their quality was compared to previously used components (standards) by expressing GFPcyc3 (4.2) and detecting its fluorescence (4.7.1). To obtain the bacterial S12 extract, the culture grown as described in 4.2.9.1 was harvested after 280 min of cultivation, when its OD_{600} reached 4.5. As intended, cells were in the exponential growth phase at this point (Fig. 15*A*). Cultivation resulted in 353 g of wet cells, a part of the cells (45%) stayed stored at -80°C and the other part served to prepare the extract (see 4.2.9.2). Extract preparation yielded 101 ml of S12 extract with the chitin binding domain tagged release factor I (CBD-RFI) and 90 ml without CBD-RFI. Removal of the CBD-RFI was verified by Western blotting using anti-CBD antibodies and the result showed that the removal was successful, as no chemiluminescent signal was detected in the S12 extract without CBD-RFI (Fig. 15*B*).

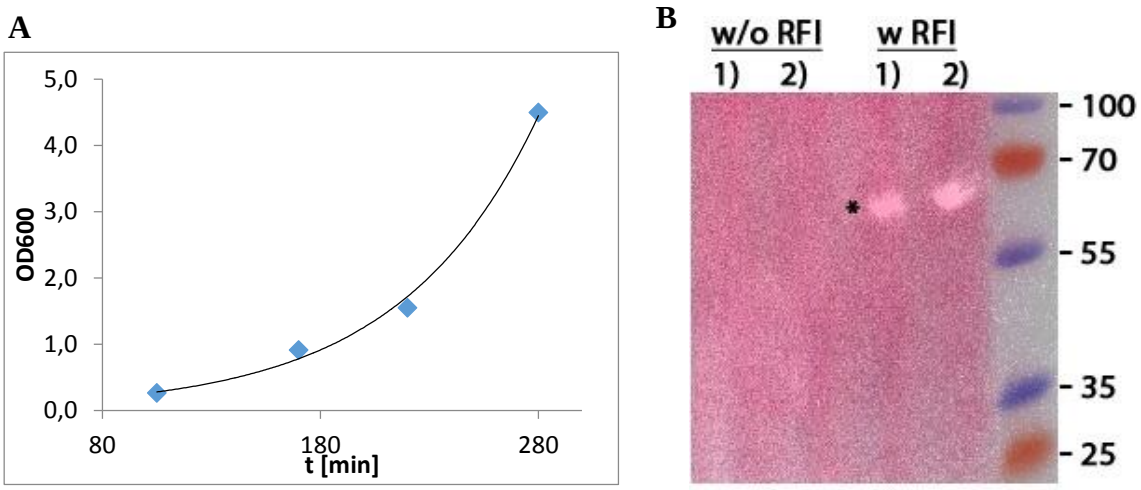

Fig. 15. (A) Growth curve of *E.coli* BL21 (DE3)::RFI-CBD$_3$ cells for S12 extract preparation monitored by OD_{600}. The obtained data approximately matches the added exponential trend line highlighting that cells were harvested in the exponential growth phase. (B) S12 Extract Western blot digitally overlaid with a picture of the same nitrocellulose membrane stained with Ponceau S. The asterisk marks the CBD-RFI (69.9 kDa) present in the S12 extract with release factor I (w RFI), but not in the S12 extract without release factor (w/o RFI). The same sample was applied twice (1, 2).

The optimal magnesium concentration for a S12 extract is generally 15-20 mM and is individual. To determine it, a series of CFPEs with 14 different magnesium concentrations (0-40 mM) was performed and the fluorescence data was evaluated using a Gaussian model (OriginPro 9.0). The calculated magnesium optimum for the S12 extract with and without CBD-RFI was 16.4 mM and 16.9 mM respectively, which was in tune with our expectations (Fig. 16*A,B*). Next, the quality of the new S12 extract with CBD-RFI was compared to the standard S12 with CBD-RFI. The fluorescence of the new S12 extract w RFI was by 27% more intense, therefore the new extract was even of better quality (Fig. 16*C*) and was used for all future CFPEs. Finally, we wanted to test if the initially introduced DNA concentration 0.01 µg/ µl was the most effective, and therefore set up CFPEs with double and half concentration of DNA. Fluorescence detection of the expressed GFPcyc3 showed that the initial DNA concentration was the most effective (Fig. 16*C*) and was then used for further experiments.

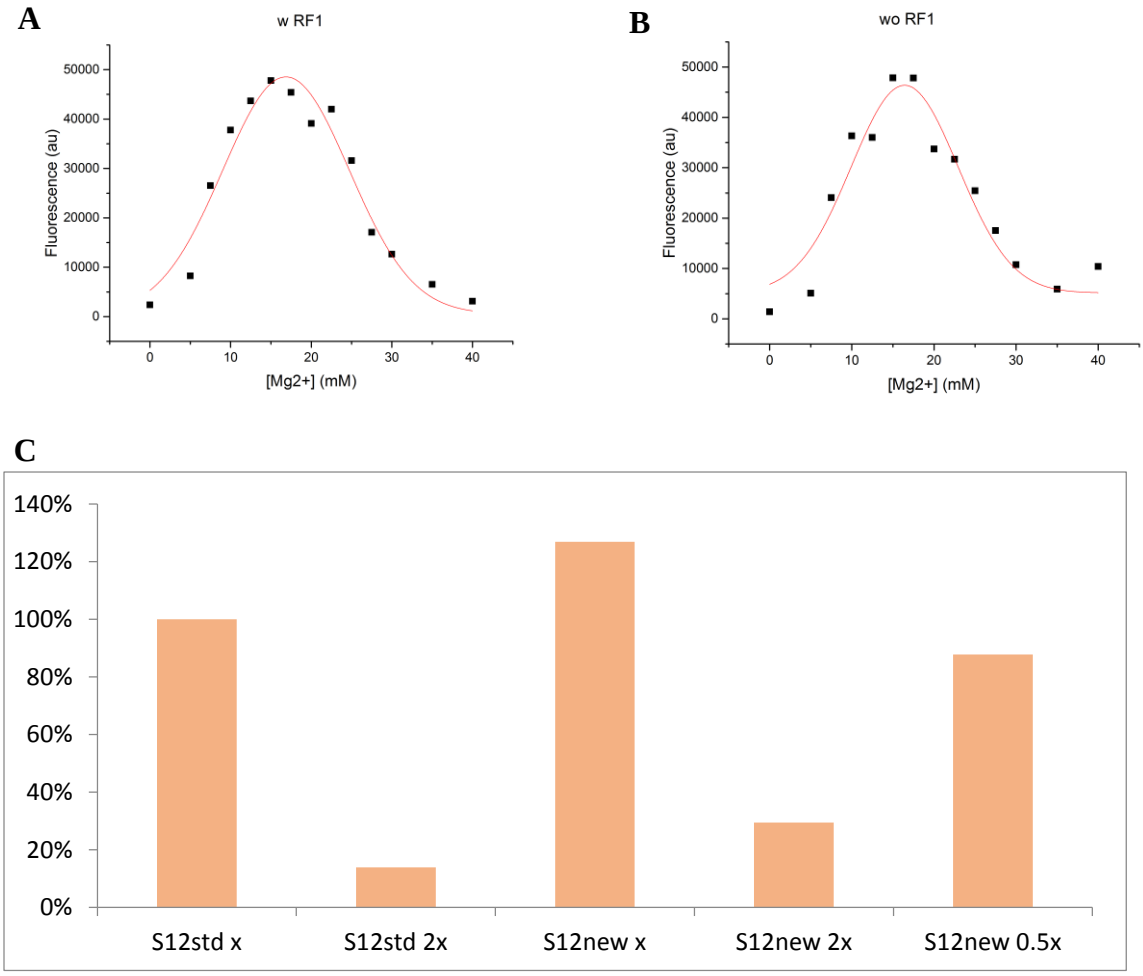

Fig. 16. (*A, B*) Determination of optimal magnesium concentration for S12 extract with CBD-RFI and without, based on GFPcyc3 fluorescence. (*C*) Comparison of new S12 extract (S12new x) to standard S12 extract (S12std x = 100% GFPcyc3). Optimal DNA concentration was verified by testing expression yield at a twice increased (2x) and decreased (0.5x) standard concentration 0.01 µg/ µl (x).

T7 expression and purification

To obtain T7, a cultivation of two one-liter cultures was performed as described in 4.2.7., and cell growth was monitored by OD_{600}. IPTG was added in the expected exponential growth phase at OD_{600}= 0.927 to flask 1 and at 1.071 to flask 2 (Fig. 17*A*), yielding 7.86 g wet cells in total. Cells were lysed and T7 was purified from the obtained supernatant by ammonium sulfate precipitation. As anticipated, the protein precipitated after adding 0.82 volumes of saturated ammonium sulfate solution and afterwards the pellet completely solubilized in buffer B. Buffer exchange was followed by ion exchange chromatography, the final purification step. The protein was eluted with a gradient from 20 mM to 1 M NaCl in buffer C. Fractions containing 38% to 62% buffer C with 1 M NaCl were collected, making a total of 62 ml eluate (Fig. 17*C*).

Eluate was concentrated to 15.8 mg/ml and the total yield was 61.62 mg protein. A SDS-PAGE analysis verified that the purified protein was T7, M.W. 99 kDa (Fig. 17*B*).

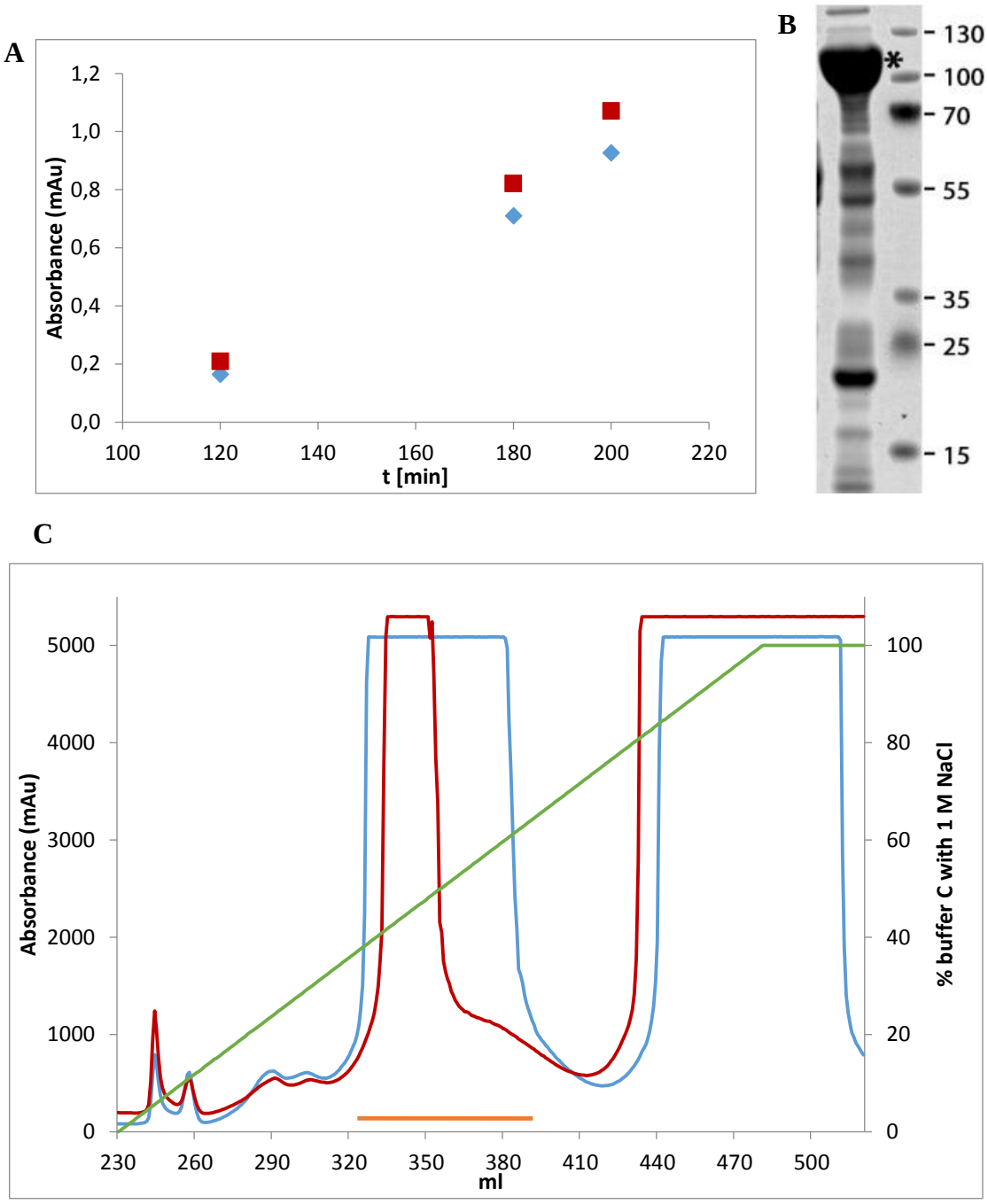

Fig. 17. (*A*) Growth of cell cultures for T7 expression (flask 1. blue, 2. red), IPTG added in the 200. minute. (*B*) A SDS-PAGE analysis of the united collected fractions containing T7 (99 kDa), marked with an asterisk. (*C*) Chromatogram from ÄKTAexplorer ion-exchange chromatography. The blue and red curve shows absorbance at 280 nm and at 260 nm respectively, the green curve corresponds to the elution gradient with buffer C containing 1 M NaCl. The orange line marks collected fractions.

All other new components (magnesium solution (Mg), low molecular weight mix (LMW), amino acid mix (AA), serine solution (Ser), glutamine solution (Gln) and T7

RNA polymerase (T7)) were compared to the standard components using the new S12 extract. New components showed equal or better expression yields, except for the T7 which was used at a 1.5x concentration in order to obtain comparable efficacy (Fig. 18).

Fig. 18. Comparison of all newly prepared components against standards (std.). Fluorescence of GFPcyc3 expressed by CFPE using standard solutions is considered as 100% and the fluorescence of GFPcyc3 expressed by CFPE using one named new solution is related to this standard.

5.3 Heterologous GPFcyc3 expression and purification

The cultivation of cells for GFPcyc3 expression was carried out as described in 4.3. The cell growth was monitored by OD_{600} in order to induce expression in the exponential growth phase. The cell culture reached OD_{600}= 0.63 after 350 min of growth and expression was then induced with 1 mM IPTG (Fig. 19*A*). Cells were harvested after 2.5 hours of expression when OD_{600} reached 1.45, and the cultivation yielded 11.67 g wet cells. After cell lyses, the His-tagged protein was purified from the supernatant by affinity chromatography on a Ni-NTA column and a SDS-PAGE sample of each purification step was taken for analysis. A SDS-PAGE gel stained with Coomassie showed the protein eluted in the predicted eluates and additionally in the 2nd wash. The M.W. of GFPcyc3 is 29.81 kDa (Fig. 19*B*). Eluates were united, dialyzed and the spectrophotometrically determined GFPcyc3 concentration was 26.8 µM. The total yield from a two liter cell culture was 187.6 nmol.

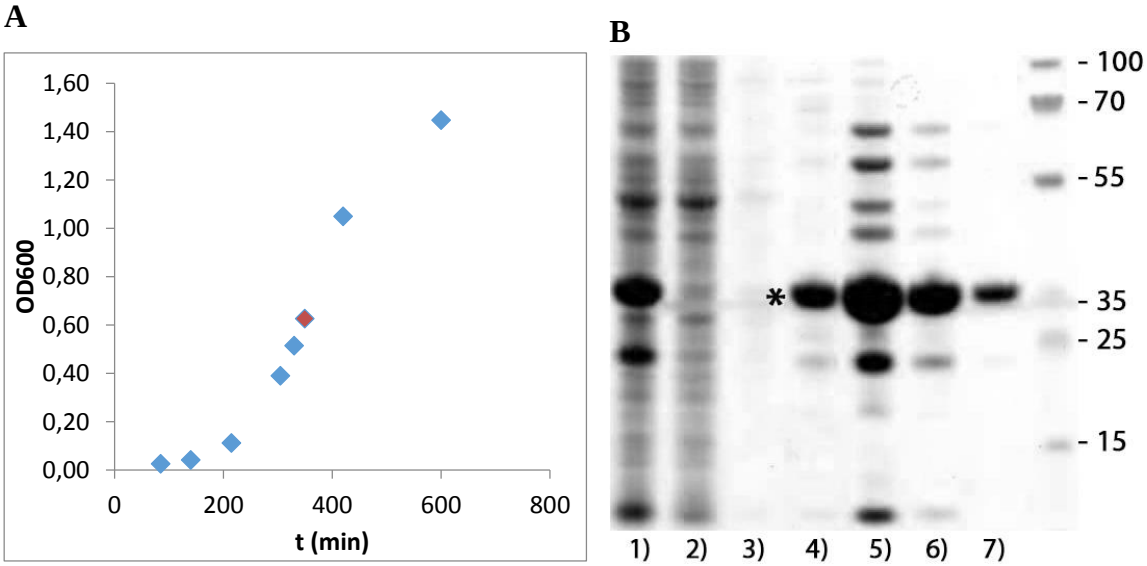

Fig. 19. (A) Growth curve of *E.Coli* BL21 Star (DE3) for GFPcyc3 expression, red dot marks IPTG induction in the exponential growth phase. (B) A SDS-PAGE analysis of GFPcyc3 purification with Coomassie staining. 1) supernatant, 2-7) purification steps on the Ni-NTA column with used imidazole concentration in brackets - 2) load (10 mM), 3) 1st wash (10 mM), 4) 2nd wash (50 mM), 5) 1st elution (150 mM), 6) 2nd elution (150 mM), 7) final elution (200 mM). Asterisk marks GFPcyc3.

5.4 Quantification of cell-free GFPcyc3 expression

To quantify GFPcyc3 expressed in a cell-free system, purified GFPcyc3 (5.3) was used to prepare five standard solutions of a known GFPcyc3 concentration (4.7.1). The slope of the corresponding GFPcyc3 fluorescence was determined by linear regression (Fig. 20), which was then used to determine the concentration of cell-free expressed GFPcyc3. This was redone for every quantification. Up to 1 µM (0.2 nmol) GFPcyc3 were obtained from a 200 µl cell-free reaction (Table 4).

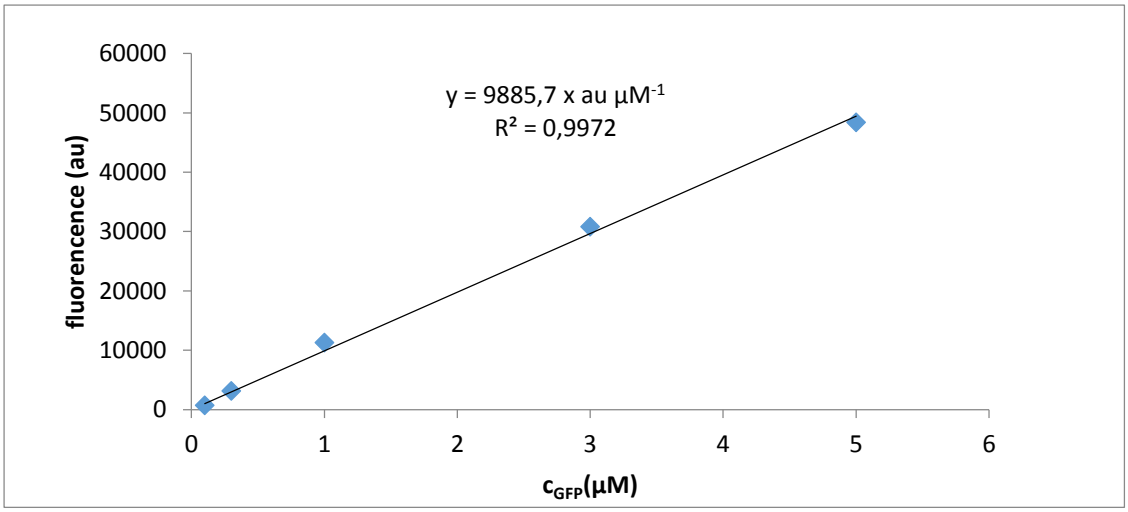

Fig. 20. Graph with the dependence of fluorescence on GFPcyc3 concentration and with the equation of the linear regression calculated from the fluorescence of five standard concentrations of GFPcyc3.

Table 4. Fluorescence of three identical samples converted to GFPcyc3 concentration using equation from Fig. 20.

	Cell-free expressed GFPcyc3			Buffer
Sample:	**1**	**2**	**3**	
fluorescence	9143	10210	10512	84
buffer correction	9059	10126	10428	0
c_{GFP} (µM)	**0.916**	**1.024**	**1.055**	
average (µM)			**0.999**	

5.5 CFPE of Na_vSp1p

We wanted to test whether it is possible to express an ion channel in a cell-free system. As Na_vSp1p is a membrane protein, a suitable detergent needed to be added for the CFPE reaction. With the selected detergents, the CFPE was performed as described in 4.2. After successful expression, we verified that the initial incubation conditions (time, temperature) were optimal.

5.5.1 Detergents

Based on literature research, we selected four nonpolar detergents (DM, DDM, Brij-58 and Brij-78, details see 4.2.2). Expression in the environment of each detergent was performed twice and additionally one expression was performed with neither DNA nor detergent to see the reaction background. To determine whether the protein was not only present, but also solubilized, samples of the total reactions and of the centrifuged supernatants were analyzed. The bands detected by Western blotting corresponded to the size of Na_vSp1p, 61.2 kDa and thereby proved that the protein had been expressed in the environment of all four detergents and also that the majority of the protein was solubilized (Fig. 21*A*, *B*).

A

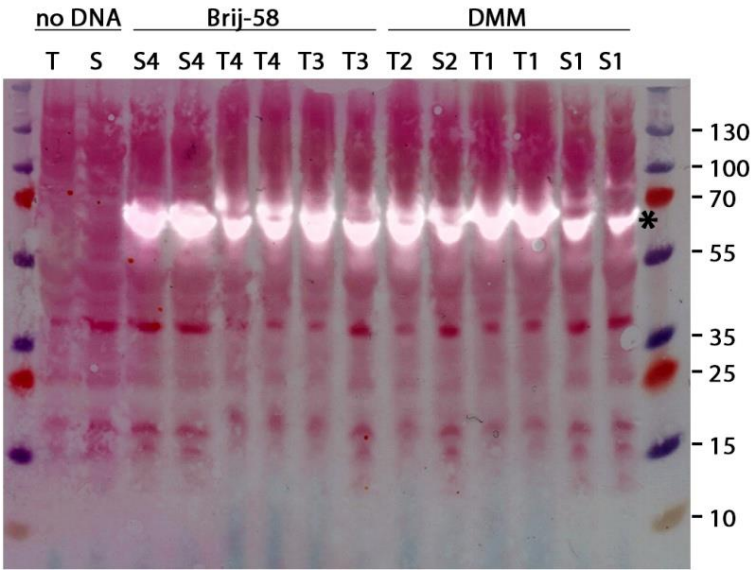

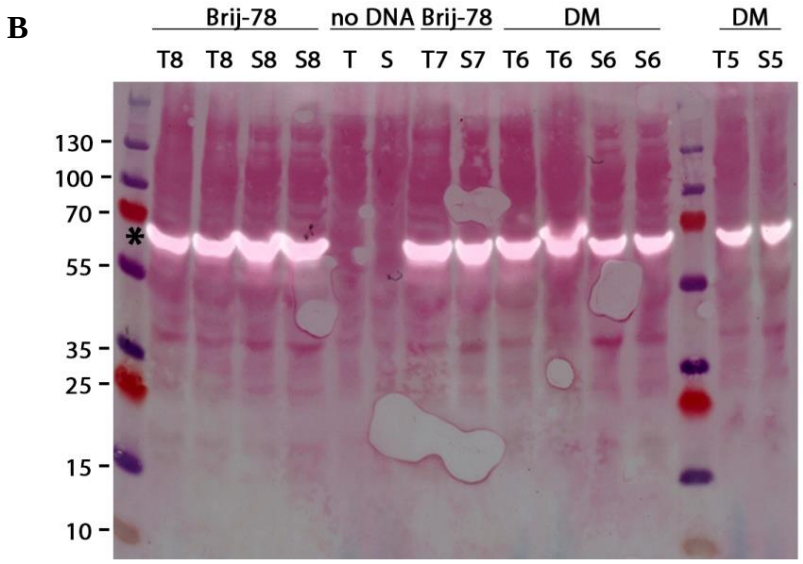

Fig. 21. Western blots of the cell-free expression of Na_vSp1p with four different detergents, digitally overlaid with a picture of the same nitrocellulose membrane stained with Ponceau S. S and T stand for supernatant and total reaction respectively. Asterisks mark Na_vSp1p. Expression in the environment of Brij-58 and DMM (*A*), and Brij-78 and DM (*B*).

5.5.2 Optimization of incubation conditions

To test if the initial expression conditions were optimal, first a different incubation temperature and second various incubation durations were tested. In the first case, expression was performed at 19°C instead of 30°C with all detergents and both total reaction and supernatants were analyzed. Result from Western blotting showed that whereas at 30°C the protein was expressed in all detergent environments, at 19°C no protein was detected in the environment of DM and DDM (Fig. 22*A*). The second experiment was performed only in the environment of Brij-78 and DM and incubation was allowed to last 2 h, 4 h and overnight. Western blot detection of both total reactions and supernatants showed that incubation time did not play a significant role in expression yield (Fig. 22*B*). As a result of these two experiments, following incubations were further carried out at 30°C for 2 h in the environment of DM, as this detergent was used in the adopted purification protocol from Shaya et al. (2011).

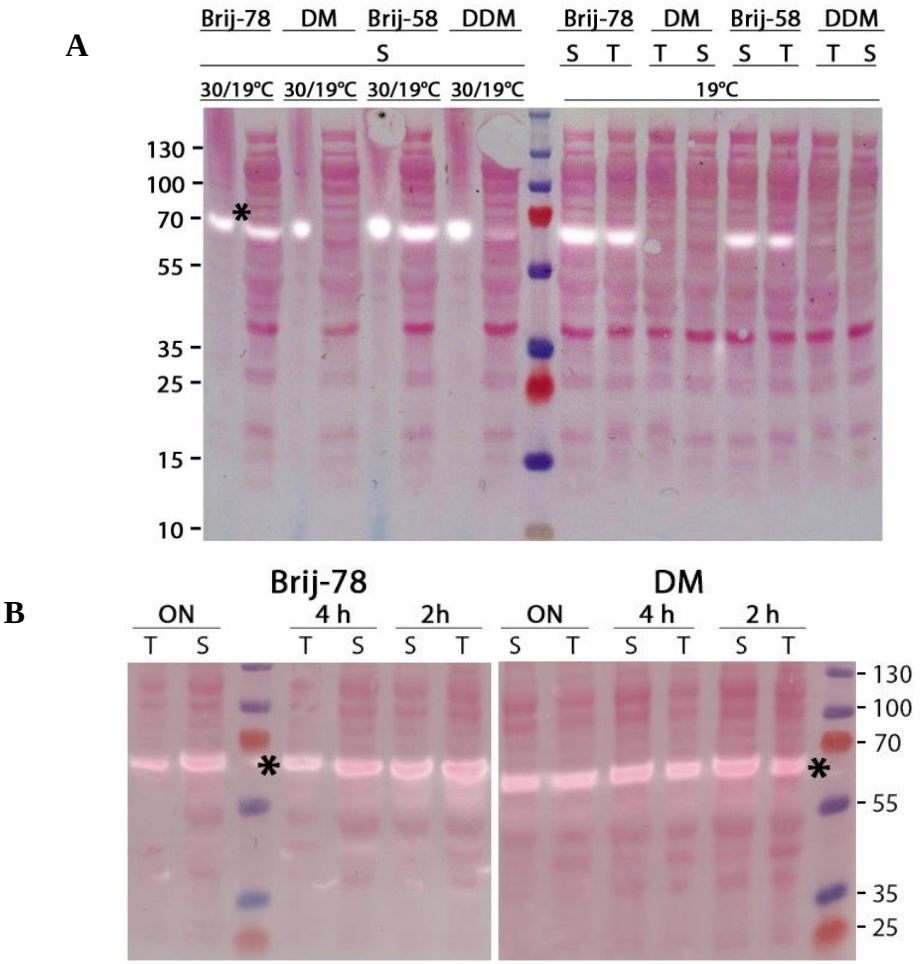

Fig. 22. Western blots of Na_vSp1p expression at various incubation conditions, digitally overlaid with a picture of the same nitrocellulose membrane stained with Ponceau S. S and T stand for supernatant and total reaction respectively. Asterisks mark Na_vSp1p. (*A*) Expression after incubation at 19°C and 30°C in the environment of all four detergents. (*B*) Expression after 2 h, 4 h and overnight (ON) incubation in Brij-78 and DM.

5.6 Purification of Na_vSp1p

Purification of the 6x His-tagged Na_vSp1p consisted of gravity-flow affinity chromatography (I. Ni-NTA), desalting (by dialysis or on a desalting column), cleavage of the 6x His-tag by HRV 3C protease, removal of the 6x His-tag, uncleaved protein and protease by gravity-flow affinity chromatography (II. Ni-NTA) and finally size exclusion chromatography (SEC). All purification steps were carried out as described in 4.4. and a sample of each purification step was taken for SDS-PAGE analysis. If desalting was performed on a HiPrep Desalting column, a typical chromatogram is shown in Fig. 23*A* where the protein elutes in the first peak and salts come in the second peak. After desalting, the protein was incubated with the 3C HRV protease and the cleaved protein (15.9 kDa) was separated from the His-tag (45.3 kDa), the protease

(47.8 kDa) and the uncleaved protein (61.2 kDa) on II. Ni-NTA. In SEC, the cleaved protein started eluting at 11 ml (Fig. 23*B*), which was in line with the expected elution volume of the tetrameric protein (67.3 kDa) according to the column product sheet. This elution volume also corresponds to the elution volume of the tetrameric protein Na_vSp1p published in Shaya et al. (2011). A SDS-PAGE analysis of collected samples verified that Na_vSp1p was successfully expressed, purified, partly cleaved and that the cleaved protein was separated from the cleavage mix (Fig. 23*C*). The yield of 30 ml of cell-free reaction was 4.4 nmol purified Na_vSp1p.

A

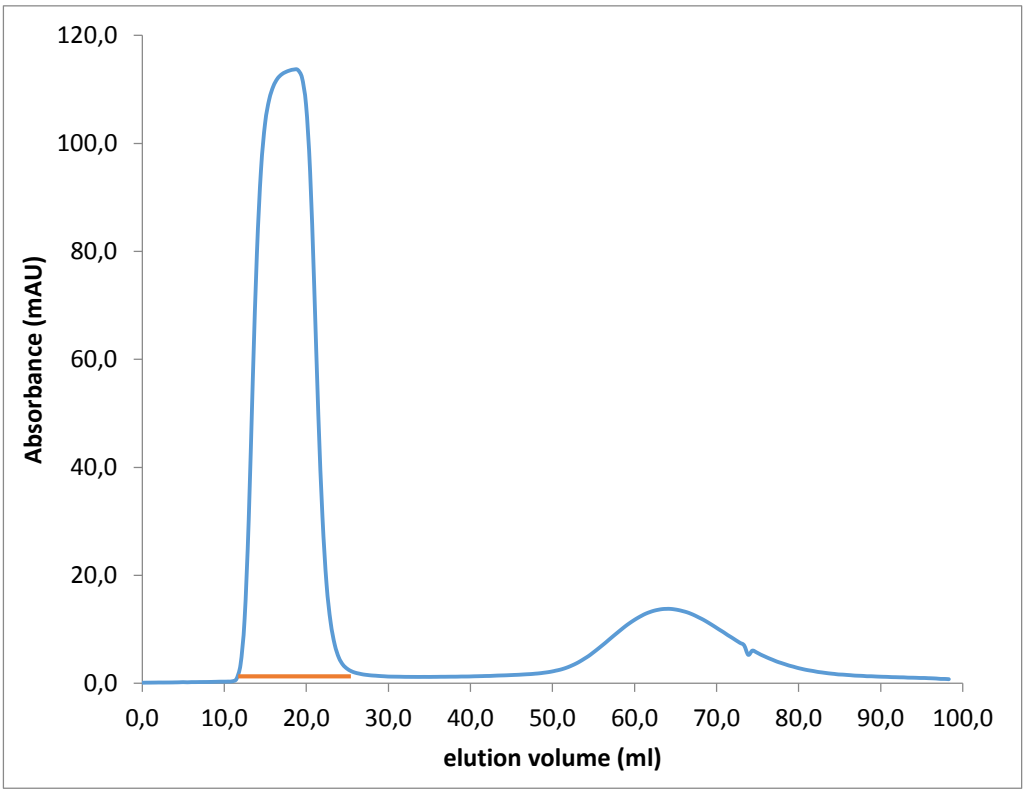

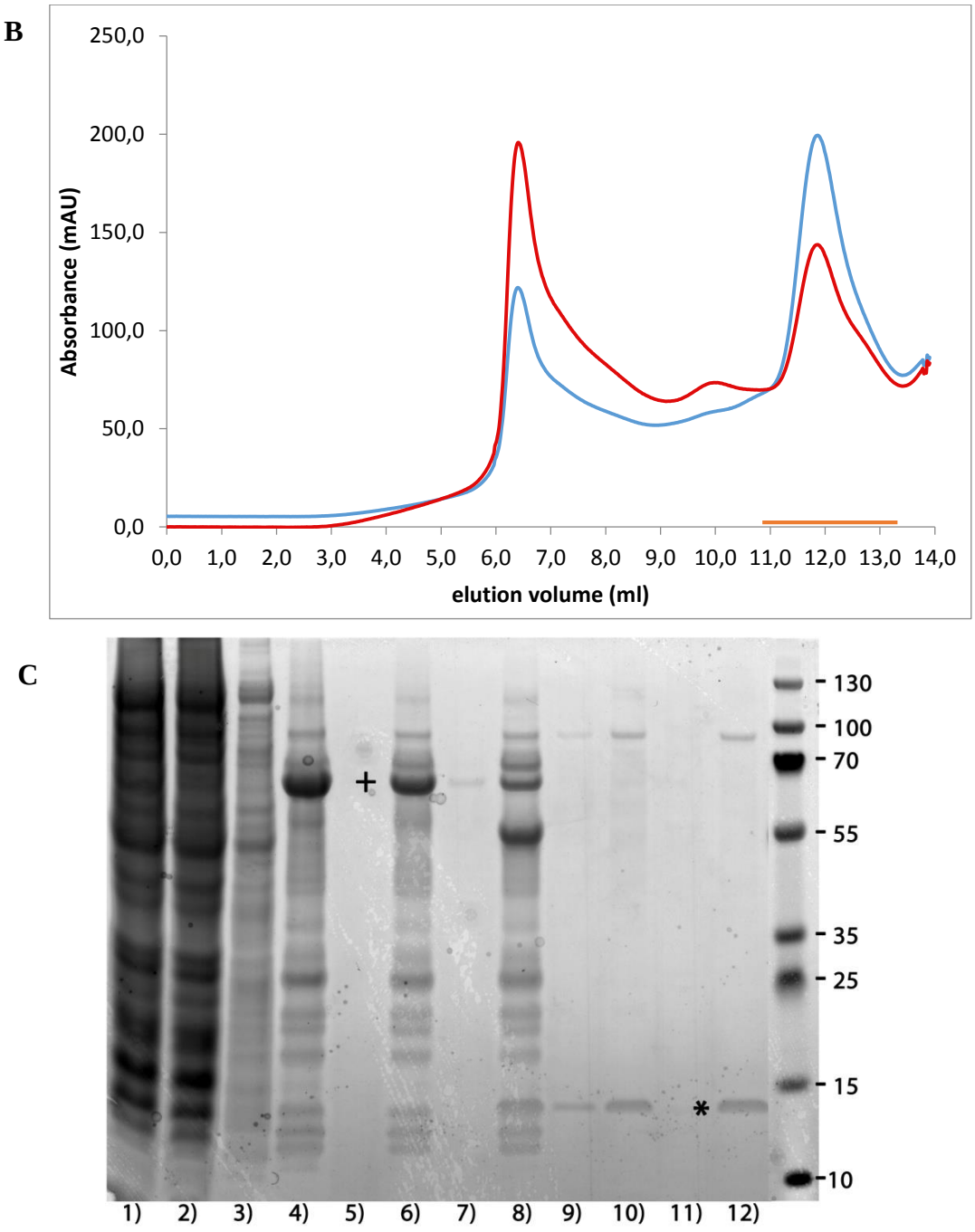

Fig. 23. Na_vSp1p purification. (*A*) Representative chromatogram from desalting by a HiPrep Desalting column. The blue curve shows absorbance at 280 nm and the orange line marks collected fractions (11.8-27 ml elution volume). (*B*) Representative chromatogram from SEC. The blue and red curve show absorbance at 280 nm and 260 nm respectively and the orange line marks collected fractions (11-13.5. ml). (*C*) SDS-PAGE analysis of selected purification steps, the gel was stained with Coomassie. The cross and the asterisk mark the full length protein and the cleaved protein respectively. 1) completed CFPE, 2-4) I. Ni-NTA steps- load, wash, eluate, 5-7) desalting – 5) fraction just prior to eluate, 6) eluate, 7) just after eluate, 8) protein and protease after incubation, 9-10) cleaved protein after II. Ni-NTA, concentrated from 16.5 ml of 9.35µM (9) to approximately 400µl of 488 µM (10), 11-12) SEC – 11) first peak, 12) second peak - collected fraction.

5.7 Optimization of protein to protease ratio for His-tag cleavage

The cleavage of the His-tag and the maltose-binding domain from the protein occurred in the environment of a detergent. Protease activity can be affected by buffer composition, especially by detergents present at a concentration above the CMC. They form a protein-detergent complex with the membrane protein and the tag can be sterically inaccessible to the protease, and therefore it is necessary to optimize cleavage conditions in the given buffer (Vergis & Wiener, 2011). We first started off with a ratio of 1:50 protease to protein. This resulted in the cleavage of only 25% of the protein (Fig. 24*A*, lane 11). Therefore we incubated the protein with different amounts of protease in order to find the optimum (ratio from 1:50 to 1:4). These experiments were analyzed by Western blotting: Increasing of protease concentration resulted in an increased protein cleavage. But even if we increased the ratio to 1:4, we still could not observe complete cleavage (Fig. 24*B*). Due to the high cost of the protease, we decided to use in future experiments ratio 1:8 protease to protein amount. Protease efficiency is often indicated in milligram instead of mol, this recalculation gave in our case a simple ratio of 1 mg of protease for 10 mg of protein, which is in line with the ratio used in the adapted protocol (Shaya et al., 2011). However, the Pierce HRV 3C protease has an approximaly 2.3 x bigger M.W. than the in-house protease used in the original protocol, and therefore we have actually used 2.3 x less protease in terms of mol.

A

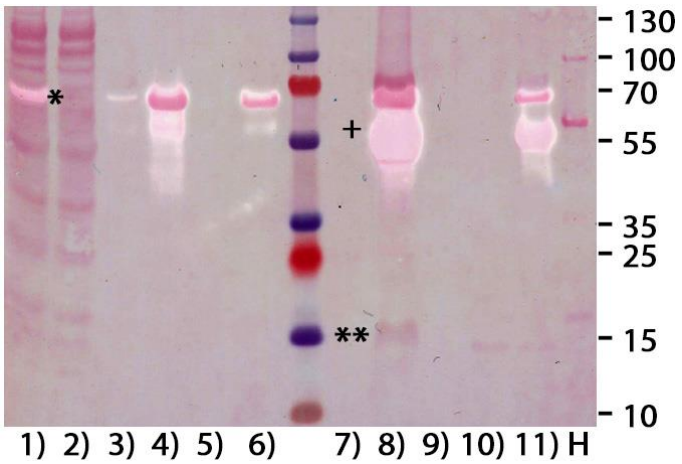

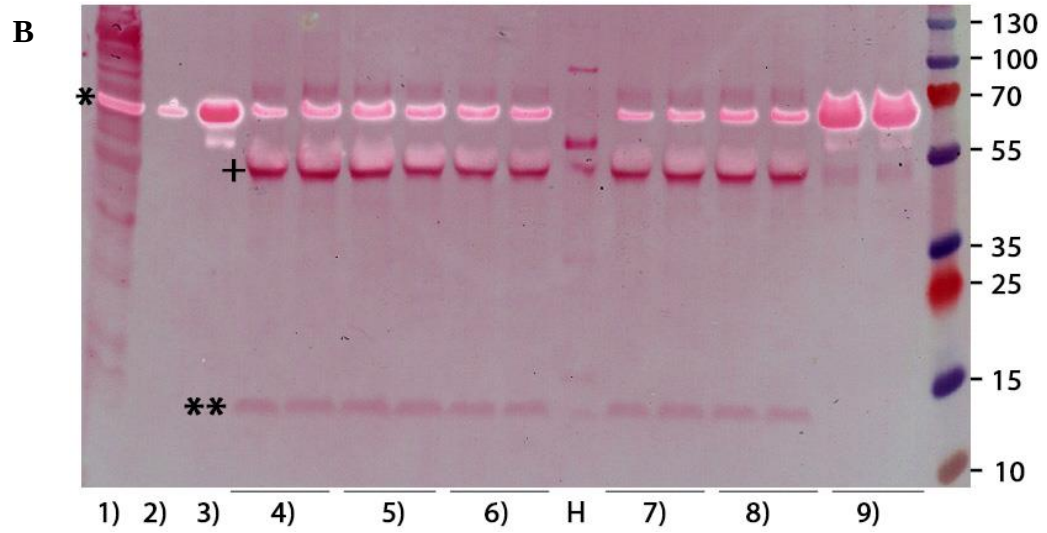

Fig. 24. A Western blot of the first Na_vSp1p purification with HRV 3C cleavage (*A*) and of Na_vSp1p incubated with 3C HRV at various ratios (*B*). The cross marks the HRV 3C, one and two asterisks mark the full length protein and the cleaved protein respectively. H indicates the His-ladder containing bands of the size 100, 75, 50, 30, 15 kDa. (*A*) 1) completed CFPE, 2-4) I. Ni-NTA steps – load, wash, eluate, 5-7) desalting – 5) fraction just prior to eluate, 6) eluate, 7) just after eluate, 8) protein and protease after incubation, 9) bottom of the concentrating tube, 10) cleaved protein after II. Ni-NTA, 11) eluted protease, His-tag and uncleaved protein from II. Ni-NTA. (*B*) 1) completed CFPE, 2-3) I. Ni-NTA eluate concentrated from 2 ml to approx. 200 µl, 9 µM, 4-9) protease to protein ratio in amount of substance 4) 1:4, 5) 1:5, 6) 1:5.5, 7) 1:8, 8) 1:16, 9) 1:50.

The cleavage in following experiments occurred at a higher rate, but the efficiency was still not satisfactory (Fig. 23*C*, lane 8). We also tested if cleavage improved in the presence of a stronger reducing agent TCEP (tris(2-carboxyethyl)phosphine) instead of DTT. Protease and protein were incubated at a ratio 1:1 (wt/wt) and TCEP was used at a final concentration 0.5 mM. SDS-PAGE analysis results did not show a visible difference in the cleavage efficiency (Fig. 25). Eventually we decided to request the vector for the HRV 3C protease in order to produce an in-house protease, so that this step would not be limiting the purification yield.

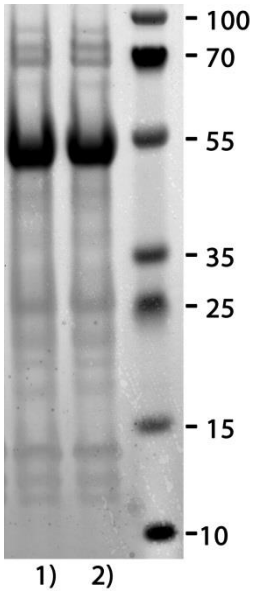

Fig. 25. A SDS-PAGE gel stained with Coomassie, depicting HRV 3C cleavage of Na_vSp1p in the environment of different reducing agents, DTT (1) and TCEP (2). Used ratio was 1:1 protease to protein (wt/wt).

5.8 HRV 3C expression and purification

Cell cultivation, expression and purification were carried out as specified in 4.5. We expected the exponential growth phase to be at OD_{600}= 0.5 and when the two one liter cultures reached OD_{600}= 0.460 and 0.550 after 295 min of growth (Fig. 26*A*), the temperature was decreased to 22°C. After 15 min, expression was induced by adding 0.4 mM IPTG and the overnight expression yielded 11.62 g wet cells. The octa-histidine tagged protein was purified by Ni-NTA affinity chromatography (Fig. 26*B*), dialyzed and centrifuged (Ti 70, 13 000 g, 40 min, 4°C) in order to remove precipitated protein. The concentration of the purified protein in the supernatant was 0.429 mM and the total yield of the purification was 7.726 mmol protein. SDS-PAGE samples of selected purification steps were taken for analysis and verified that HRV 3C, M.W. 21. 282 kDa, was expressed and purified (Fig. 26*C*,*D*).

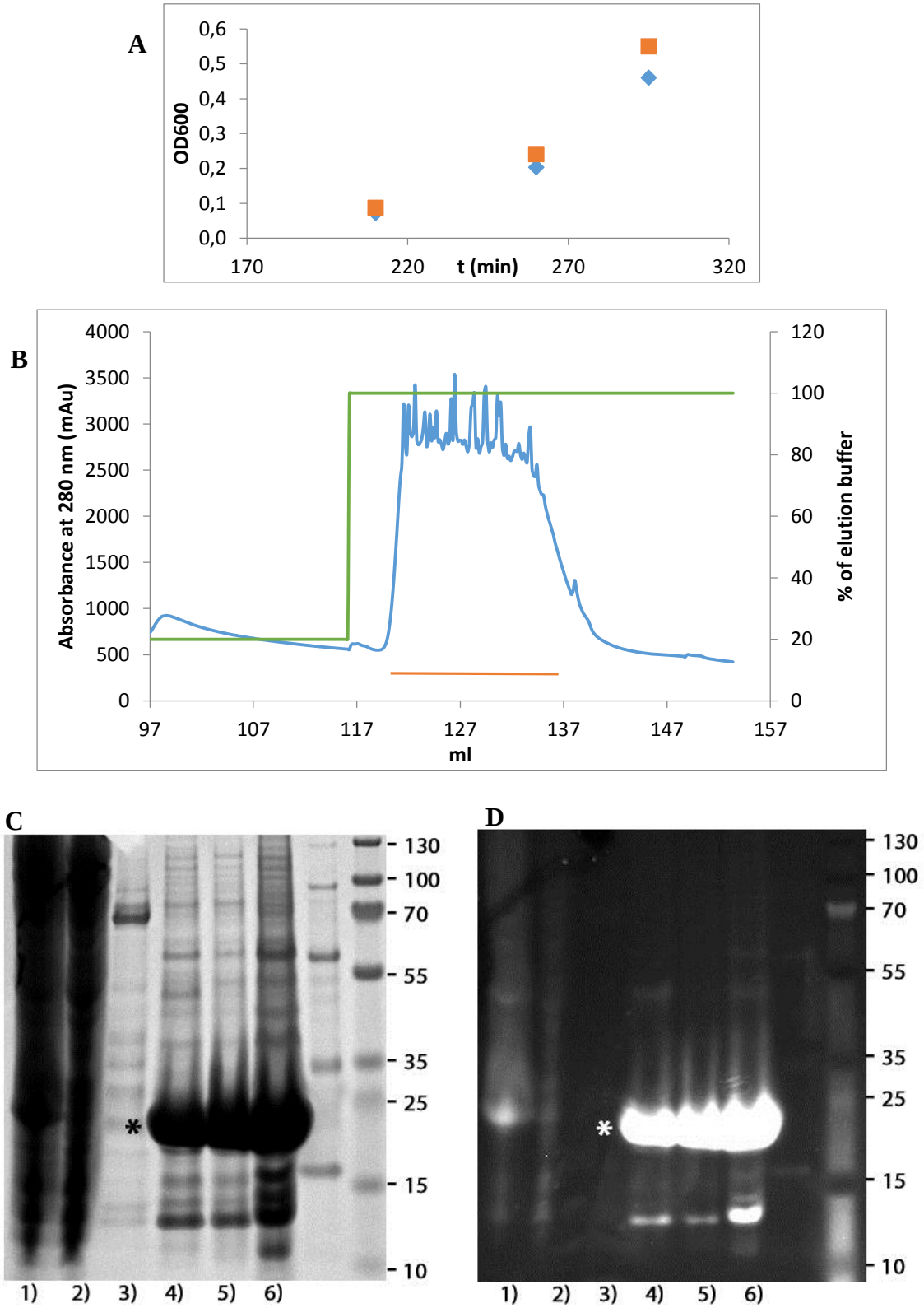

Fig. 26. (*A*) Growth of *E.coli* BL21 Star cultures for 3C HRV expression (flask 1. blue, 2. red). (*B*) Chromatogram from Ni-NTA affinity chromatography. The blue curve shows absorbance at 280 nm, the green curve corresponds to the amount of elution buffer and the orange line marks collected fractions. (*C-D*) SDS-PAGE analysis of selected purification steps, 3C HRV is marked with an asterisk. 1) supernatant from lysate, 2-4) Ni-NTA affinity chromatography – 2) flow-through after loading column, 3) wash 4) collected fractions, 5) centrifuged protein after dialysis, 6) resuspended precipitate after dialysis. The gel was stained with Coomassie (*C*) and InVision™ His-tag In-gel Stain (*D*).

5.8.1 Functionality assay

We wanted to test the functionality of the new in-house HRV 3C protease compared to the purchased Pierce protease. For this purpose the protease was incubated with the control GST-Syk protein as described in 4.5.1 and results were detected by a SDS-PAGE analysis. Uncleaved GST-Syk protein had a M.W. of 54 kDa and is cleaved by the 3C HRV into a 26 kDa and 28 kDa protein (information on GST-Syk protein provided by the Thermo Scientific technical support). In-house purified HRV 3C had a M.W. of 21.28 kDa and purchased Pierce HRV 3C was 48.7 kDa. Evaluation of the SDS PAGE gel stained both with InVision™ His-tag In-gel Stain and Coomassie showed, that 0.022 nmol in-house purified 3C HRV cleaved 0.093 nmol GST-Syk protein as efficiently as 0.021 nmol Pierce 3C HRV (Fig. 27*A,B*). This result shows that the same amount of in-house protease cleaved the control protein as efficiently as the Pierce HRV 3C protease. This implicates the in-house protease is fully functional and can replace the Pierce HRV 3C protease in all future experiments.

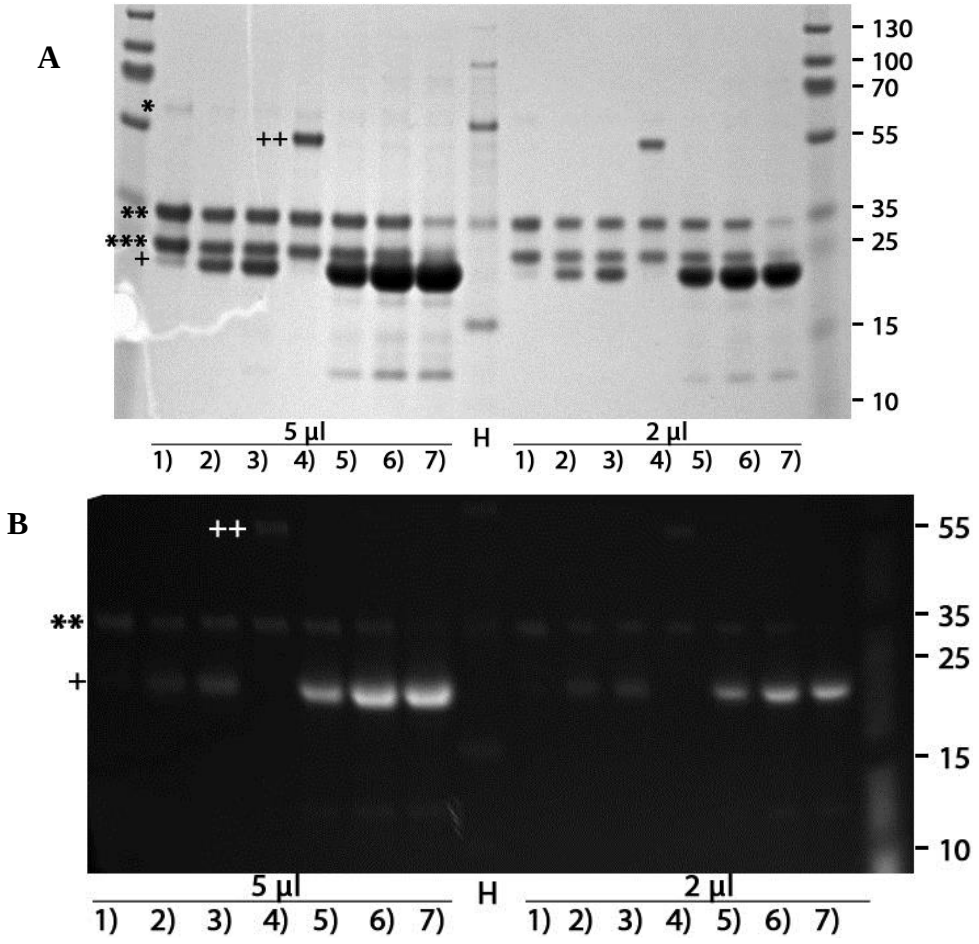

Fig. 27. 3C HRV functionality assay. GST-Syk protein was incubated with the in-house 3C HRV at various ratios (Table 2.). One asterisk marks the uncleaved GST-Syk protein, two and three asterisks mark products of the digestion. In-house HRV 3C is marked with a cross, purchased HRV 3C with two

crosses. H indicates the His-ladder containing bands of the size 100, 75, 50, 30, 15 kDa. Volume of sample is indicated in µl. Samples are denoted as protease:protein ratio- 1) 1:4.3, 2) 1:0.43, 3) 1:0.22, 4) Pierce 1:4.4, 5) 1:0.043, 6) 1:0.011, 7) 1:0.0043. (*A*) Coomassie and (*B*) InVision staining.

5.9 IR spectrum of Na_vSp1p

The quantity of Na_vSp1p we purified was not optimal for a FTIR measurement, but we still expected to detect a moderate signal. To obtain an approximate spectrum of the protein from the collected data, we multiplied the protein spectrum so that the vibration frequencies of water were of similar absorbance in both the buffer spectrum and the protein spectrum. Then we subtracted the absorbance of the buffer from the multiplied spectrum of the protein in buffer and we obtained the two bands typical for protein spectrums, amide I (1600- 1700 cm^{-1}) and amide II (~1550 cm^{-1}) (Fig. 28). Amide I band mirrors the secondary structure of the protein (Baiz et al., 2012), and in our case, the peak of amide I is at 1650 cm^{-1} which aptly corresponds to the alpha helical structure of Na_vSp1p. Though due to the necessary significant corrections, this experiment has to be redone.

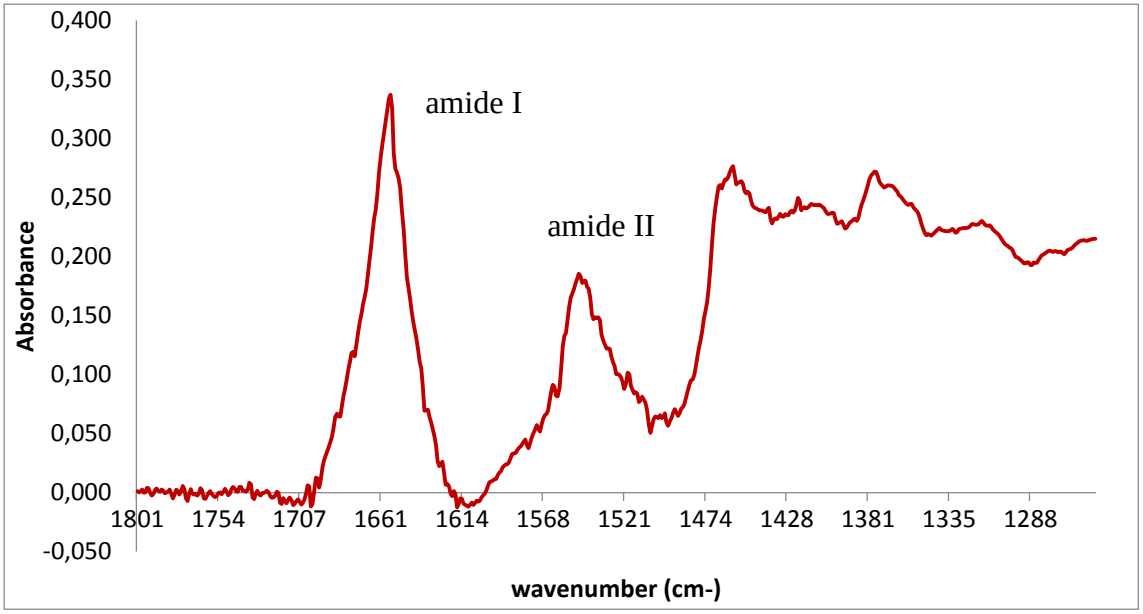

Fig. 28. Corrected FTIR spectra of Na_vSp1p. Spectrum of the Na_vSp1p was multiplied by 12 and then the spectrum of the buffer was subtracted. Amide I (1600- 1700 cm^{-1}) and amide II (~1550 cm^{-1}) vibrations of the polypeptide backbones are marked.

5.10 Mutation of the channel

We selected three amino acids from the selectivity filter which are likely to play a significant role in the ion selectivity of the channel and performed three single amino acid mutations so that an isotope labeled amino acid can be inserted instead of the natural amino acid (4.6). We mutated S177, because it is highly conserved among bacterial Na_v and it was observed that a mutation to D alters selectivity to calcium over sodium by 200-fold. Second, we are interested in the role of L175 as it is conserved among both bacterial sodium and calcium channels (Shaya et al., 2013). The third selected amino acid was G181, because glycine residues are absolutely conserved in the K^+ channels selectivity filter and it was revealed that this only not chiral amino acid was essential for the correct structure and function of the selectivity filter (Valiyaveetil et al., 2004), all shown in Fig. 29.

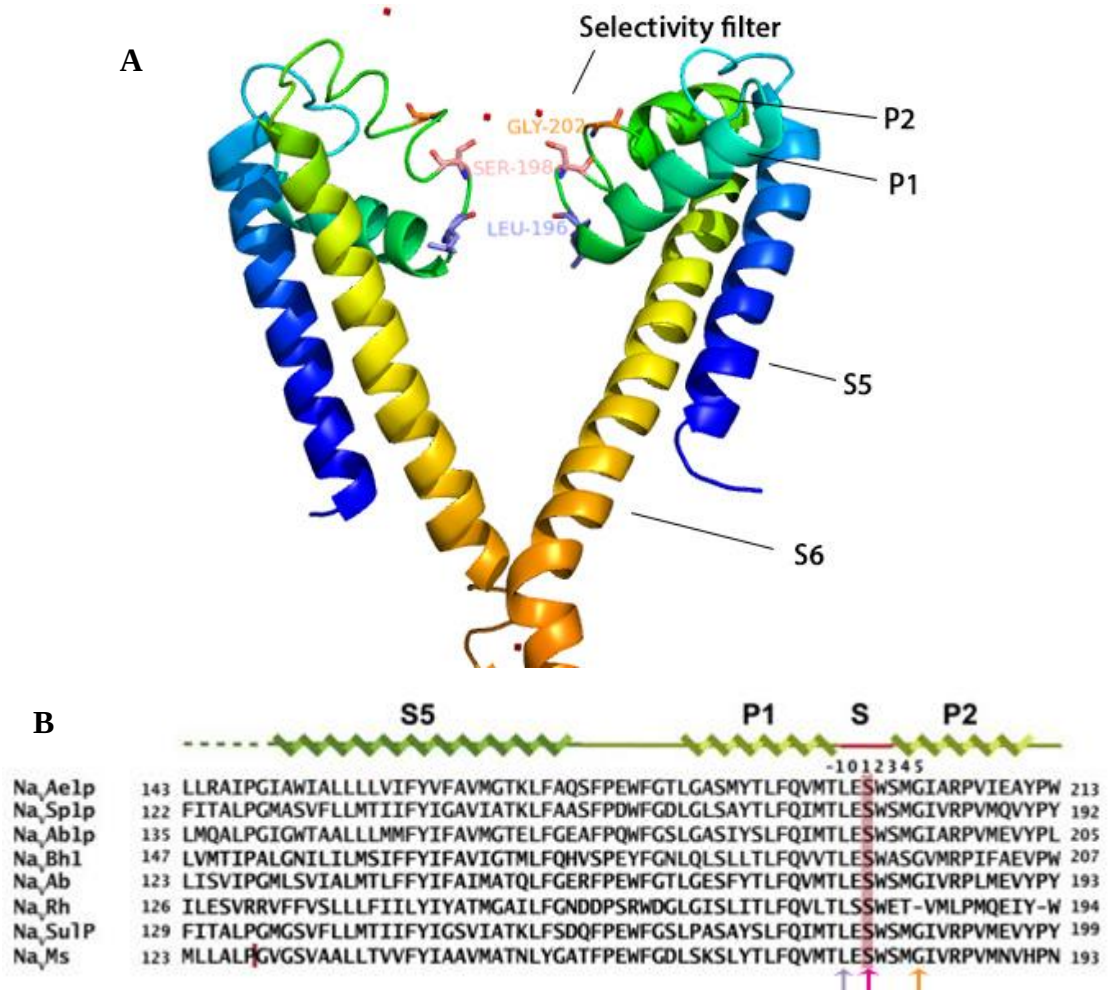

Fig. 29. *(A)* A cross-section of the recently determined structure of Na_vAe1p, a close relative of Na_vSp1p. The side chains of amino acids Gly202, Ser198 and Leu196 which are homologous to the ones we mutated in Na_vSp1p, are shown as sticks and labeled. This Pymol picture was created from the PDB

coordinate file 4LTO, Na_vAe1p, crystal I, high calcium and only two opposing domains formed by the two transmembrane helices (S5, S6) are shown. The selectivity filter positioned in the outer pore between loops P1 and P2 is indicated. ***(B)*** Sequence alignment of closely related bacterial Na_vs demonstrating the highly conserved selectivity filter (S) with arrows pointing at mutated amino acids. Adapted from Shaya et al. (2013).

Three agarose plates were inoculated with one mutant obtained from PCR each. After incubation (12 h, 37°C), four single colonies of each mutant were picked and DNA was purified and digested (4.2.10) in order to select which samples were to be sent for DNA sequencing (Fig. 30).

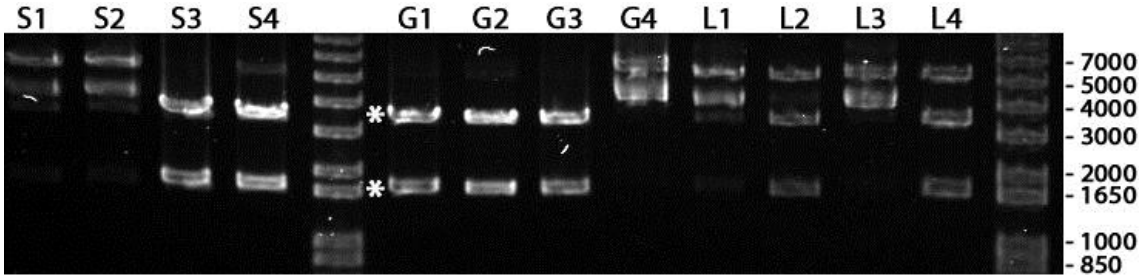

Fig. 30. Restriction enzyme analysis of four Na_vSp1p DNA samples from each mutant. Fragments from a successful digestion are marked with an asterisk. Clones sent for sequencing were S3, S4 for S177 mutants, G1, G2, G3 for G181 mutants and L2, L4 for L175 mutants.

Sequencing confirmed that we possessed at least one positive clone of each mutation for future use:

```
piVEX24d_Nav TCTGTCGGCCTATACGCTGTTCCAGATCATGACGCTGGAAAGCTGGTCGATGGGCATC - 2400
Nav_G181_G1  TCTGTCGGCCTATACGCTGTTCCAGATCATGACGCTGGAAAGCTGGTCGATGTAGATC - 510

piVEX24d_Nav TCTGTCGGCCTATACGCTGTTCCAGATCATGACGCTGGAAAGCTGGTCGATGGGCATC - 2400
Nav_L175_L2  TCTGTCGGCCTATACGCTGTTCCAGATCATGACGTAGGAAAGCTGGTCGATGGGCATC - 547

piVEX24d_Nav GTCTGTCGGCCTATACGCTGTTCCAGATCATGACGCTGGAAAGCTGGTCGATGGGCAT - 2399
Nav_S177_S3  GTCTGTCGGCCTATACGCTGTTCCAGATCATGACGCTGGAATAGTGGTCGATGGGCAT - 504
```

6 DISCUSSION

We established a cell-free expression of the prokaryotic pore-only sodium channel Na_vSp1p and its subsequent purification. As shown by SDS-PAGE and Western blotting (5.5, 5.6), we observe pure protein which elutes as tetramer from the gel filtration column (5.6). Even though the functionality of an ion channel can only be demonstrated by electrophysiological recordings, the tetrameric assembly is a good indication that we actually got a functional ion channel. The ultimate goal of this project is to study ion selectivity by means of 2D IR spectroscopy which requires about 50 to 100 nmol protein for an experiment. Is it possible to get that much NavSp1p? The largest batch that we successfully set up and purified NavSp1p from was a 30 ml CFPE reaction yielding 4.4 nmol protein (5.6). This is about 10 to 25 times less than what is needed. For reasons like practicability and costs scaling up of the reaction is only possible to some extent. Therefore an improvement in the purification protocol is necessary for obtaining a sufficient amount of protein.

To purify the protein, we modified the purification protocol for Na_vSp1p expressed *in vivo* in *E.coli* cells published by Shaya et al. (2011). As in the original protocol, we first used immobilized metal ion affinity chromatography (IMAC) to extract the protein from the reaction mixture. However, we used only 20 mmol imidazole in the wash buffer instead of the 50 mmol, because otherwise the protein eluted already in the washing step. The sample was desalted and then cleaved from the tag by the HRV 3C protease. Next, the His-tag, the uncleaved protein and the His-tagged protease were removed by a second IMAC. We omitted the removal of 1 mM DTT that had been added to the cleavage mixture, because the Ni-NTA agarose is compatible with up to 10 mM DTT. Furthermore, we decided neither to remove traces of MBP nor to perform ion exchange chromatography prior to the final purification step, a gel filtration (4.4). SDS-PAGE analysis showed that this simplified protocol yielded purified protein (5.6).

The bottle neck of the current protocol is the cleavage of the fusion protein by the HRV 3C protease for two reasons. First, the cleavage is far from being complete (Fig. 23*C*) and about four times more NavSp1p could be observed by increasing the amount of protease. This leads to the second point, cost of the protease. To observe 4.4 nmol NavSp1p, 108 nmol fusion protein was cut with 620 µl protease which cost 316 €. To

keep the costs of the experiment reasonable, we decided to acquire HRV 3C protease DNA and to set up its expression and purification. Within this project, the in-house protease was expressed, purified (5.8) and the functionality confirmed by cleaving a control protein (5.8.1). With this unlimited supply in protease it should be possible to obtain from the 30 ml CFPE producing 108 nmol fusion protein about 22 nmol of purified NavSp1p after encountering losses due to cleavage, second IMAC, gel filtration and protein concentration. Therefore it is necessary to start with about 100 to 150 ml CFPE to do 2D IR experiments. This will be quite some effort but it is surely possible.

In the 2D IR spectroscopy experiments the ion selectivity of voltage-gated sodium channel will be investigated. A similar 2D IR experiment has been designed by the Vaziri Group, who study the ion selectivity of the prokaryotic potassium channel KcsA, using the model peptide valinomycin. The direct observation of the ion interaction in the KcsA protein is still hampered by the lack of experimental techniques to produce site-specifically isotope-labeled proteins.
The Westenhoff lab is currently working on establishing a generic method to achieve this using a cell-free expression system combined with artificially produced tRNAs which introduce the isotope label in response to amber stop codons. Based on the crystal structure of a homologue ion channel we have identified several sites that are most likely involved in the ion selectivity of sodium channels (5.10) and produced the DNA with the corresponding sites mutated to amber codons. However, it seems as if the sodium channel does not strip of all the water molecules that are in direct contact with the sodium ion. This might lead to experimental difficulties in observing the ion – side chain interactions since the strength of the interactions is weaker, but bear also the potential to identify whether the water molecules are actually bound to the ion or rather to the protein. Nonetheless, this can be only shown in future experiments.

7 CONCLUSION

This work demonstrates expression and purification of Na_vSp1p as a preparation for future 2D IR experiments aimed at investigating the ion selectivity of a voltage-gated sodium channel.

Within my Master project I completed the following:

(1) I prepared components for cell-free protein expression and tested their quality by green fluorescent protein expression, which showed that all components were functional, and in some cases the new components were of better quality than the previous.

(2) Cell-free expression of the Na_vSp1p was achieved and optimal expression conditions (detergent, time, temperature) were determined.

(3) I elaborated a protocol for the purification of Na_vSp1p by modifying a purification protocol for *in vivo* expressed Na_vSp1p published by Shaya et al. (2011). Furthermore, in-house expression and purification of a functional HRV 3C protease was established in order to increase the purification yield and to keep costs reasonable. A preliminary IR spectrum of Na_vSp1p was recorded.

(4) Based on the crystal structure of a homologue ion channel, amino acids which are likely to contribute to ion selectivity were selected and DNA mutants enabling future 2D IR experiments were prepared.

8 ABBREVIATIONS

ATB	antibiotics
AMP	ampicillin
bp	base pair
Ca_v	voltage-gated calcium channel
CBD-RFI	chitin binding domain tagged release factor 1
CMC	critical micelle concentration
CV	column volume
DDM	n-dodecyl-ß-D-maltoside
DM	n-decyl-β-D-maltoside
DTT	dithiothreitol
EDTA	ethylenediaminetetraacetic acid
g	gravitational acceleration if related to centrifugation, otherwise gram
GFP	green fluorescent protein
GFPcyc3	green fluorescent protein cycle 3 mutant
IMAC	immobilized metal ion affinity chromatography
IPTG	isopropyl-β-D-thiogalactopyranoside
IR	infrared
kDa	kilo Dalton
K_v	voltage-gated potassium channel
LB	lysogeny broth
MBP	maltose binding protein
MES	2-(*N*-morpholino)ethanesulfonic acid
MP	membrane protein
M.W.	molecular weight
MWCO	molecular weight cut off
NaChBac	voltage-gated sodium channel from *Bacillus halodurans*
NaPi	phosphate buffer
Na_v	voltage-gated sodium channel
Ni-NTA	agarose beads with a modified nitrilotriacetic acid chelating Ni^+
OD_{600}	optical density at 600 nm
PMSF	phenylmethanesulfonylfluoride
RF1	release factor 1

rpm	rotations per minute
SEC	size exclusion chromatography
SDS-PAGE	sodium dodecyl sulphate-polyacrylamide gel electrophoresis
TAE buffer	tris-acetate-EDTA buffer
TTX	tetrodotoxin
UAAs	unnatural amino acids
VGIC	voltage-gated ion channel
wt/wt	weight to weight ratio

9 BIBLIOGRAPHY

AccuRapid™ Cell-Free protein expression kit. (n.d.). Retrieved April 01, 2014, from http://us.bioneer.com/products/protein/Cell-FreeProteinExpressionKit-technical.aspx

Baiz, C. R., Reppert, M., & Tokmakoff, A. (2012). Introduction to Protein 2D IR Spectroscopy, (22), 1–38.

Cantrell, A. R., & Catterall, W. A. (2001). Neuromodulation of Na+ channels: an unexpected form of cellular plasticity. *Nature Reviews. Neuroscience*, *2*(6), 397–407. doi:10.1038/35077553

Catterall, W. A. (1986). Voltage-dependent gating of sodium channels: correlating structure and function. *Trends in Neurosciences*, *9*, 7–10. doi:10.1016/0166-2236(86)90004-4

Catterall, W. A. (2000). From Ionic Currents to Molecular Mechanisms. *Neuron*, *26*(1), 13–25. doi:10.1016/S0896-6273(00)81133-2

Clapham, D. E., & Garbers, D. L. (2005). International Union of Pharmacology. L. Nomenclature and structure-function relationships of CatSper and two-pore channels. *Pharmacological Reviews*, *57*(4), 451–4. doi:10.1124/pr.57.4.7

Clare, J. J., Tate, S. N., Nobbs, M., & Romanos, M. A. (2000). Voltage-gated sodium channels as therapeutic targets. *Drug Discovery Today*, *5*(11), 506–520. Retrieved from http://www.sciencedirect.com/science/article/pii/S1359644600015701

Crameri, A., Whitehorn, E. A., Tate, E., & Stemmer, W. P. (1996). Improved green fluorescent protein by molecular evolution using DNA shuffling. *Nature Biotechnology*, *14*(3), 315–9. doi:10.1038/nbt0396-315

Davanloo, P., Rosenberg, a H., Dunn, J. J., & Studier, F. W. (1984). Cloning and expression of the gene for bacteriophage T7 RNA polymerase. *Proceedings of the National Academy of Sciences of the United States of America*, *81*(7), 2035–9. Retrieved from http://www.ncbi.nlm.nih.gov/pmc/articles/PMC345431/pdf/pnas00608-0112.pdf

Direct Detect, Analytical chemistry. (n.d.). Retrieved March 28, 2014, from http://www.analyticalchemistrygsu.com/2012/03/new-assay-technique-introducing-direct.html

Fourier Transform Infrared Spectrometry, Intertek. (n.d.). Retrieved April 06, 2014, from http://www.ptli.com/testlopedia/tests/FTIR-E168andE1252-more.asp

Guy, H. R., & Seetharamulu, P. (1986). Molecular model of the action potential sodium channel. *Proceedings of the National Academy of Sciences of the United States of America*, *83*(2), 508–12. Retrieved from

http://www.pubmedcentral.nih.gov/articlerender.fcgi?artid=322889&tool=pmcentrez&rendertype=abstract

Hamm, P., & Zanni, M. (2011). *Concepts and Methods of 2D Infrared Spectroscopy* (1st ed., p. 286). New York: Cambridge University Press.

Heinemann, S. H., Terlau, H., Stühmer, W., Imoto, K., & Numa, S. (1992). Calcium channel characteristics conferred on the sodium channel by single mutations. *Nature*, *356*(6368), 441–3. doi:10.1038/356441a0

Hille, B. (2001). . In *Ion Channels of Excitable Membranes* (pp. 1–22). Sunderland, MA: Sinauer Associates, Inc. Retrieved from http://pub.ist.ac.at/Pubs/courses.migrated/2012/introductiontoneuroscience1/docs/Lectures May 13,15/Hille_Ion Channels of Excitable Membranes_Chapter1.pdf

Hodgkin, A. L., & Huxley, A. F. (1952). A quantitative description of membrane current and its application to conduction and excitation in nerve. *The Journal of Physiology*, *117*(4), 500–44. Retrieved from http://www.pubmedcentral.nih.gov/articlerender.fcgi?artid=1392413&tool=pmcentrez&rendertype=abstract

InVision™ His-tag In-gel Stain, User Guide. (n.d.). Retrieved March 30, 2014, from http://tools.lifetechnologies.com/content/sfs/manuals/invisionstain_man.pdf

Isaksson, L., Enberg, J., Neutze, R., Göran Karlsson, B., & Pedersen, A. (2012). Expression screening of membrane proteins with cell-free protein synthesis. *Protein Expression and Purification*, *82*(1), 218–25. doi:10.1016/j.pep.2012.01.003

Kapust, R. B., & Waugh, D. S. (1999). Escherichia coli maltose-binding protein is uncommonly effective at promoting the solubility of polypeptides to which it is fused. *Protein Science : A Publication of the Protein Society*, *8*(8), 1668–74. doi:10.1110/ps.8.8.1668

Kaupp, U. B., & Seifert, R. (2002). Cyclic Nucleotide-Gated Ion Channels. *Physiol Rev*, *82*(3), 769–824. Retrieved from http://physrev.physiology.org/content/82/3/769

Koishi, R., Xu, H., Ren, D., Navarro, B., Spiller, B. W., Shi, Q., & Clapham, D. E. (2004). A superfamily of voltage-gated sodium channels in bacteria. *The Journal of Biological Chemistry*, *279*(10), 9532–8. doi:10.1074/jbc.M313100200

Loscha, K. V, Herlt, A. J., Qi, R., Huber, T., Ozawa, K., & Otting, G. (2012). Multiple-site labeling of proteins with unnatural amino acids. *Angewandte Chemie (International Ed. in English)*, *51*(9), 2243–6. doi:10.1002/anie.201108275

Mantegazza, M., Curia, G., Biagini, G., Ragsdale, D. S., & Avoli, M. (2010). Voltage-gated sodium channels as therapeutic targets in epilepsy and other neurological disorders. *The Lancet Neurology*, *9*(4), 413–424. Retrieved from http://www.sciencedirect.com/science/article/pii/S1474442210700594

McCusker, E. C., Bagnéris, C., Naylor, C. E., Cole, A. R., D'Avanzo, N., Nichols, C. G., & Wallace, B. A. (2012). Structure of a bacterial voltage-gated sodium channel pore reveals mechanisms of opening and closing. *Nature Communications*, *3*, 1102. doi:10.1038/ncomms2077

McCusker, E. C., D'Avanzo, N., Nichols, C. G., & Wallace, B. a. (2011). Simplified bacterial "pore" channel provides insight into the assembly, stability, and structure of sodium channels. *The Journal of Biological Chemistry*, *286*(18), 16386–91. doi:10.1074/jbc.C111.228122

Payandeh, J., Gamal El-Din, T. M., Scheuer, T., Zheng, N., & Catterall, W. A. (2012). Crystal structure of a voltage-gated sodium channel in two potentially inactivated states. *Nature*, *486*(7401), 135–9. doi:10.1038/nature11077

Payandeh, J., Scheuer, T., Zheng, N., & Catterall, W. A. (2011). The crystal structure of a voltage-gated sodium channel. *Nature*, *475*(7356), 353–8. doi:10.1038/nature10238

Pedersen, A., Hellberg, K., Enberg, J., & Karlsson, B. G. (2011). Rational improvement of cell-free protein synthesis. *New Biotechnology*, *28*(3), 218–224. Retrieved from http://www.sciencedirect.com/science/article/pii/S1871678410004917

Pless, S. A., Galpin, J. D., Frankel, A., & Ahern, C. A. (2011). Molecular basis for class Ib anti-arrhythmic inhibition of cardiac sodium channels. *Nature Communications*, *2*, 351. doi:10.1038/ncomms1351

QuikChange® Site-Directed Mutagenesis Kit, Instruction Manual. (2013). Retrieved March 29, 2014, from http://kirschner.med.harvard.edu/files/protocols/Stratagene_quickchangepdf.pdf

Ren, D., Navarro, B., Xu, H., Yue, L., Shi, Q., & Clapham, D. E. (2001). A prokaryotic voltage-gated sodium channel. *Science (New York, N.Y.)*, *294*(5550), 2372–5. doi:10.1126/science.1065635

Sang, C. N., Bennett, G. J., Bhattacharya, A., Wickenden, A. D., & Chaplan, S. R. (2009). Sodium Channel Blockers for the Treatment of Neuropathic Pain. *Neurotherapeutics*, *6*(4), 663–678. Retrieved from http://www.sciencedirect.com/science/article/pii/S1933721309001329

Shaya, D., Findeisen, F., Abderemane-Ali, F., Arrigoni, C., Wong, S., Nurva, S. R., … Minor, D. L. (2013). Structure of a Prokaryotic Sodium Channel Pore Reveals Essential Gating Elements and an Outer Ion Binding Site Common to Eukaryotic Channels. *Journal of Molecular Biology*. Retrieved from http://www.sciencedirect.com/science/article/pii/S0022283613006360

Shaya, D., Kreir, M., Robbins, R. a, Wong, S., Hammon, J., Brüggemann, A., & Minor, D. L. (2011). Voltage-gated sodium channel (NaV) protein dissection creates a set of functional pore-only proteins. *Proceedings of the National Academy of Sciences of the United States of America*, *108*(30), 12313–8. doi:10.1073/pnas.1106811108

Schwarz, D., Klammt, C., Koglin, A., Löhr, F., Schneider, B., Dötsch, V., & Bernhard, F. (2007). Preparative scale cell-free expression systems: new tools for the large scale preparation of integral membrane proteins for functional and structural studies. *Methods (San Diego, Calif.)*, *41*(4), 355–69. doi:10.1016/j.ymeth.2006.07.001

Valiyaveetil, F. I., Sekedat, M., Mackinnon, R., & Muir, T. W. (2004). Glycine as a D-amino acid surrogate in the K(+)-selectivity filter. *Proceedings of the National Academy of Sciences of the United States of America*, *101*(49), 17045–9. doi:10.1073/pnas.0407820101

Vaziri Group. (n.d.). Coupled Dynamics & Protein Function. Retrieved April 28, 2014, from http://vaziria.com/?page_id=320

Venkatachalam, K., & Montell, C. (2007). TRP channels. *Annual Review of Biochemistry*, *76*, 387–417. doi:10.1146/annurev.biochem.75.103004.142819

Vergis, J. M., & Wiener, M. C. (2011). The variable detergent sensitivity of proteases that are utilized for recombinant protein affinity tag removal. *Protein Expression and Purification*, *78*(2), 139–142. Retrieved from http://www.sciencedirect.com/science/article/pii/S1046592811001033

Yu, F., & Catterall, W. (2003). Overview of the voltage-gated sodium channel family. *Genome Biology*, *4*(3), 207. doi:10.1186/gb-2003-4-3-207

Zhang, X., Ren, W., DeCaen, P., Yan, C., Tao, X., Tang, L., … Yan, N. (2012). Crystal structure of an orthologue of the NaChBac voltage-gated sodium channel. *Nature*, *486*(7401), 130–4. doi:10.1038/nature11054

Zhang, X., Xia, M., Li, Y., Liu, H., Jiang, X., Ren, W., … Gong, H. (2013). Analysis of the selectivity filter of the voltage-gated sodium channel Na(v)Rh. *Cell Research*, *23*(3), 409–22. doi:10.1038/cr.2012.173